# FINAL REPORT

for

# "CONSTRUCTION AND TESTING OF A SPACE READY RECTENNA"

Work performed for

## NASA LEWIS RESEARCH CENTER

under

## GRANT NAG 3-1368

by

## THE CENTER FOR SPACE POWER
## TEXAS ENGINEERING EXPERIMENT STATION
## THE TEXAS A&M UNIVERSITY SYSTEM



Prepared by
Alan M. Brown

## Microwave Energy Transmission in Space (METS) Rectenna

In February, 1993, the Solar Power Satellite (SPS) Working Group from ISAS, Japan will launch a sounding rocket into low earth orbit to perform two activities: 1) collect scientific information on the high power microwave - ionosphere interaction, and 2) demonstrate microwave power transmission in space at 2.45 GHz. The SPS Working Group announced an open invitation to international agencies willing to collaborate with the METS experiment in a number of categories. Under the sponsorship of the NASA's Lewis Research Center, the Center for Space Power located at Texas A&M University joined the experiment by producing a microwave rectifying receiving antenna (rectenna).

The rectenna is special type of receiving antenna with unique properties and characteristics. The rectenna's main purpose is to efficiently convert microwave power into DC power. The rectenna is an advanced component in microwave power beaming technology developed for 2.45 GHz. The state-of-the-art rectenna for this frequency consists of dipole antennas, filter circuits, and transmission lines etched on a thin layer of Kapton film. The format of the thin film rectenna is ideally suited for space applications. Thin film rectennas have a low specific mass of approximately 1 kg/kW [1]. The main component of the rectenna is the rectifying diode. High conversion efficiencies (90%) in microwave to DC power are capable with special Schottky barrier diodes correctly located in the rectenna circuitry [2].

This document will explain the theory of operation of the 2.45 GHz rectenna. Experimental test results on the METS rectenna will be presented. The packaging of the rectenna will also be discussed to meet space qualifications.

**Theory:**

The rectenna element can be divided into three parts: 1) the antenna, 2) the rectifying circuitry, and 3) the DC transmission line and resistive load. All three areas will be addressed theoretically using antenna and circuit theory. Unique aspects of the rectenna will also be pointed out.

The antenna used for receiving the microwave energy is a $\lambda/2$ dipole where $\lambda$ is the free space wavelength (12.24 cm at 2.45 GHz). The dipole is located approximately a $\lambda/4$ above a reflecting plane. The input impedance of the dipole under this configuration is approximately 120 $\Omega$ [3]. Resonance of the dipole is obtained by shorting the length of the dipole to approximately 0.475 $\lambda$. The gap length between the dipole terminals is determined by the separation of the balanced transmission lines. The characteristic impedance of the coplanar stripline determines this separation.

The antenna configuration was selected based on the radiation pattern of a $\lambda/2$ dipole located $\lambda/4$ over a reflector. The radiation patterns produced by a single horizontal dipole placed $\lambda/4$ above the ground plane are shown in Figure 1 [4]. The broken lines represent the dipole antenna located in free space. Under this arrangement, no sidelobes are produced as seen by the side and front views. This characteristic is important for the efficient reception of microwave power.

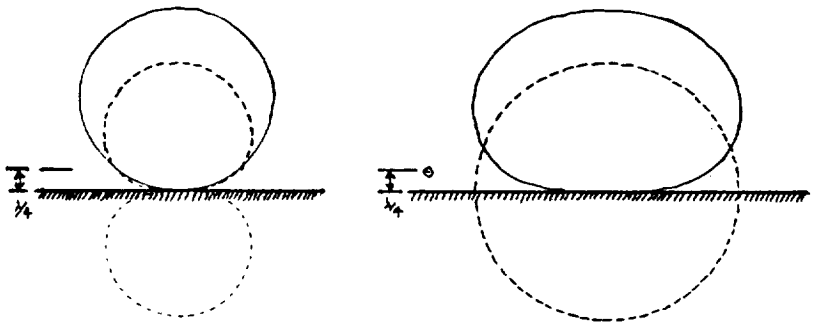

Figure 1. Radiation patterns of a $\lambda/2$ dipole located a $\lambda/4$ above a ground plane. The broken lines are the pattern without the reflecting plane.

The rectenna elements are connected by a common transmission line. Each rectenna element has a diode to convert the microwave power to DC power and filters on both sides of the diode. Essentially, each rectenna element is RF isolated from their neighboring elements even though they are physically connected by transmission lines. Theoretically the collection efficiency is 100% when no reradiation from the rectenna illuminates into sidelobes and all radiation occurs in the main beam of the rectenna [5]. Experimental evidence has shown to support this theory by the detection of an almost unity standing wave ratio in front of the rectenna [6]. Even though it appears to be a

phased array of dipole antennas, the patterns produced by the rectenna essentially resemble a single element. Thus, the rectenna is basically non-directive and ideal for receiving power for airborne vehicles that pitch and roll.

The antenna terminals feed directly into a two section low pass filter. The low pass filter performs three tasks: 1) impedance match the input impedance of the dipole to the input impedance to the diode, 2) pass the 2.45 GHz operating frequency and attenuate the higher order harmonics produced by the diode, and 3) act as a tank circuit for the on and off cycles of the diode.

The filter design is based on the constant k type of low pass filters [3]. The low pass filter is divided into two sections where the phase shift through each section is 90° at 2.45 GHz. The impedance transforming property of each section is governed by

$$Z_i = \frac{Z_o^2}{Z_t} \tag{1}$$

where $Z_i$ is the input impedance to the filter, $Z_0$ is the characteristic impedance of the filter section, and $Z_t$ is the terminating impedance. The format of the filter sections can either be T or $\pi$. The $\pi$ format is selected for the rectenna which allows the calculations to be performed easier in admittances. The general format of the $\pi$ network is shown in Figure 2.

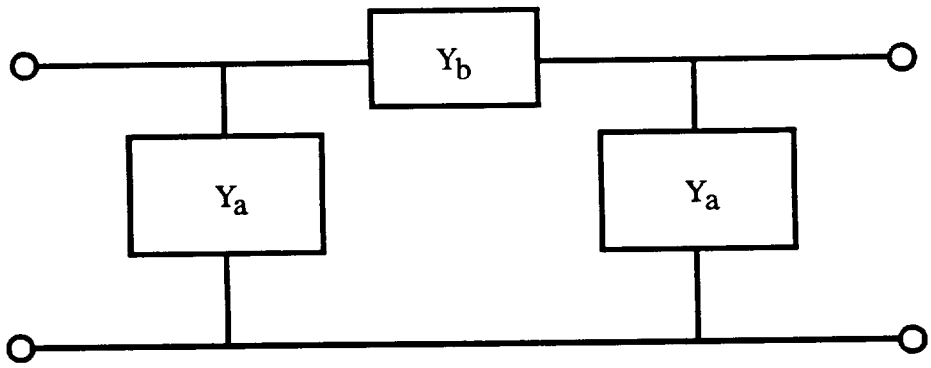


Figure 2. Equivalent $\pi$ network of rectenna transmission line.

The expressions for the loss-free transmission line are shown in Figure 3.

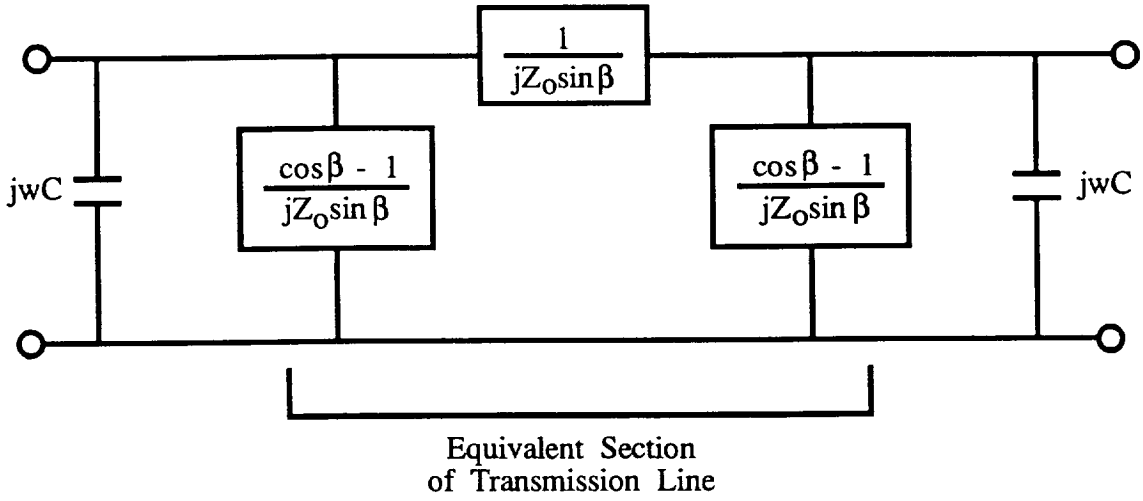


Figure 3. General network expressions for a lossless transmission line.

The parameter β is the electrical length of the transmission line section and is calculated as

$$\beta = \frac{2\pi L}{\lambda} = \frac{2\pi f L}{c} \tag{2}$$

where L is the physical length of the transmission line, λ is the free space wavelength, f is the frequency, and c is the velocity of light. The characteristic impedance of the transmission line is given by $Z_o$. The characteristic admittance and phase of figures 2 and 3 are given by:

$$Y_o = \sqrt{Y_{11}^2 - Y_{12}^2} \tag{3}$$

and

$$\theta = \cos^{-1}\left(\frac{-Y_{22}}{Y_{12}}\right) \tag{4}$$

where

$$Y_{11} = Y_a + Y_b = Y_{22} \tag{5}$$

$$Y_{12} = -Y_b \tag{6}$$

Using these equations and Figure 3 to solve for the characteristic admittance, the calculations are equated as follows:

$$\begin{aligned} Y_{11} &= j\omega C + \frac{\cos\beta - 1}{jZ_o\sin\beta} + \frac{1}{jZ_o\sin\beta} \\ &= j\omega C + \frac{\cos\beta}{jZ_o\sin\beta} \end{aligned} \tag{7}$$

$$Y_{12} = -\frac{1}{jZ_o\sin\beta} \tag{8}$$

Then

$$Y_o = \sqrt{\left(j\omega C + \frac{\cos\beta}{jZ_o\sin\beta}\right)^2 - \left(\frac{-1}{jZ_o\sin\beta}\right)^2} \tag{9}$$

Because the phase shift of each section is 90°, equation (4) can be calculated as

$$-\omega C Z_o \sin\beta + \cos\beta = 0 \tag{10}$$

which can be reduced to

$$\cot\beta = \omega C Z_o \tag{11}$$

Substituting equation (11) into (9), the characteristic admittance is obtained as

$$Y_o = \sqrt{\omega^2 C^2 + \frac{1}{Z_o}} \tag{12}$$

The capacitors used on the low pass filter are calculated from equation (12) as

$$C_x = \sqrt{\frac{Y_{ox}^2 - Y_o^2}{\omega^2}} \tag{13}$$

where $Y_{ox}$ represents the characteristic admittance of the two sections. The two sections are denoted as $Y_{o1}$ and $Y_{o2}$ and the corresponding capacitors are denoted as $C_1$ and $C_2$.

The impedance transformation of the low pass filter sections matches the dipole input impedance of 120 Ω to the diode input impedance of 270 Ω. Each section has its own characteristic impedance.

The first section has a characteristic impedance of 120 Ω to match the dipole input impedance. The capacitors of this section are denoted as $C_1$. By the use of equation (13) with $Z_{o1}$ equal to 120 Ω and $Z_o$ equal to 270 Ω, $C_1$ is calculated to be 0.485 pF at 2.45 GHz. The length of this section is calculated by equation (11) by solving for β and using $C_1$ as the capacitor value. The length of the first section is 0.461 radians or 8.97 mm at 2.45 GHz.

The second section has a characteristic impedance of 180 Ω. The capacitors of this section are denoted as $C_2$. By use of equation (13) with $Z_{o2}$ equal to 180 Ω and $Z_o$ equal to 270 Ω, $C_2$ is 0.269 pF at 2.45 GHz. The length of this section is calculated to be 0.73 radians or 14.21 mm by use of equation (11).

The circuit schematic drawing is shown in Figure 4. The two adjacent capacitors, C1 and $C_2$, form one capacitor when adding the values in parallel. Thus, the value of this second capacitor is 0.754 pF.

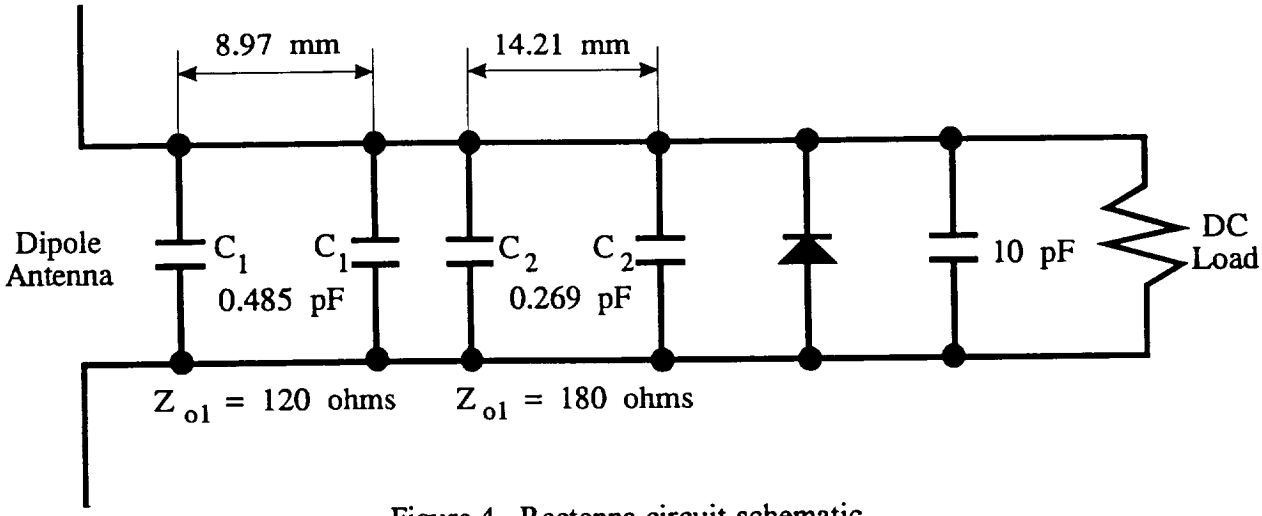


Figure 4. Rectenna circuit schematic.

The circuit was simulated by EESof's Touchstone microwave circuit software and the result is shown in Figure 5. At 2.45 GHz, the phase shift is 180° as seen by ANG[S21] and the signal is totally transmitted as noted by DB[S21]. At the second harmonic value of 4.9 GHz, the attenuation is greater than 20 dB. This simulation is for ideal (lossless) transmission lines.

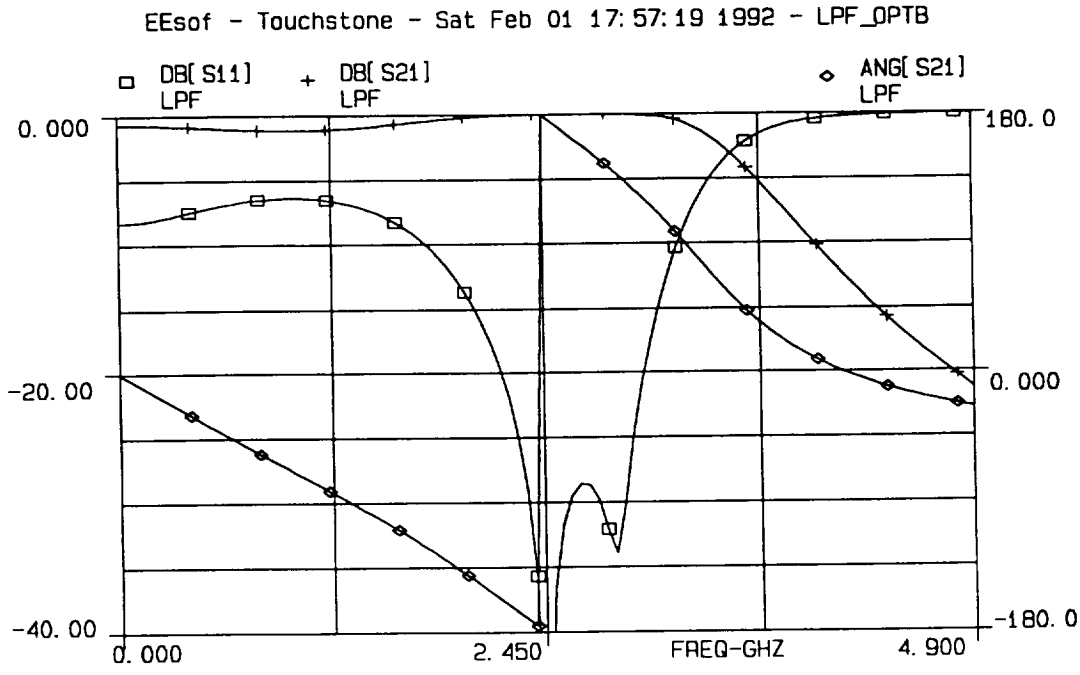


Figure 5. Simulation of constant k low pass filter.

Physical implementation of the circuit design involves the elimination of the third capacitor. The third capacitor is replaced by the diode which produces an effective capacitance [7]. The dimensions of the capacitor patches are determined by

$$\text{Area} = \frac{h\,C}{\varepsilon_r\,\varepsilon_0} \tag{14}$$

where h is the substrate height, C is twice the capacitor value computed from equation (13), $\varepsilon_r$ is the dielectric constant of the substrate, and $\varepsilon_0$ is $8.854 \times 10^{-12}$ F/m. Because the capacitors are halved on each side of the coplanar stripline, the capacitance is determined by adding the halves in series. Therefore, the capacitance used in equation (14) is twice the value calculated from equation (13). The substrate is Type F Kapton made by DuPont with FEP Teflon used as the laminate for the copper. The thickness of the Kapton film is 1 mil and the Teflon coating is 0.5 mil thick on both sides. The dielectric constant of the Kapton film with the Teflon coating was experimentally discovered to be 3.09 at 2.45 GHz and the loss tangent to be 0.0033 [7]. Using the substrate thickness of 2 mils and dielectric constant of 3.09, the area of the capacitors under the coplanar stripline are calculated by equation (14). The printed circuit and dimensions are shown in Figure 6.

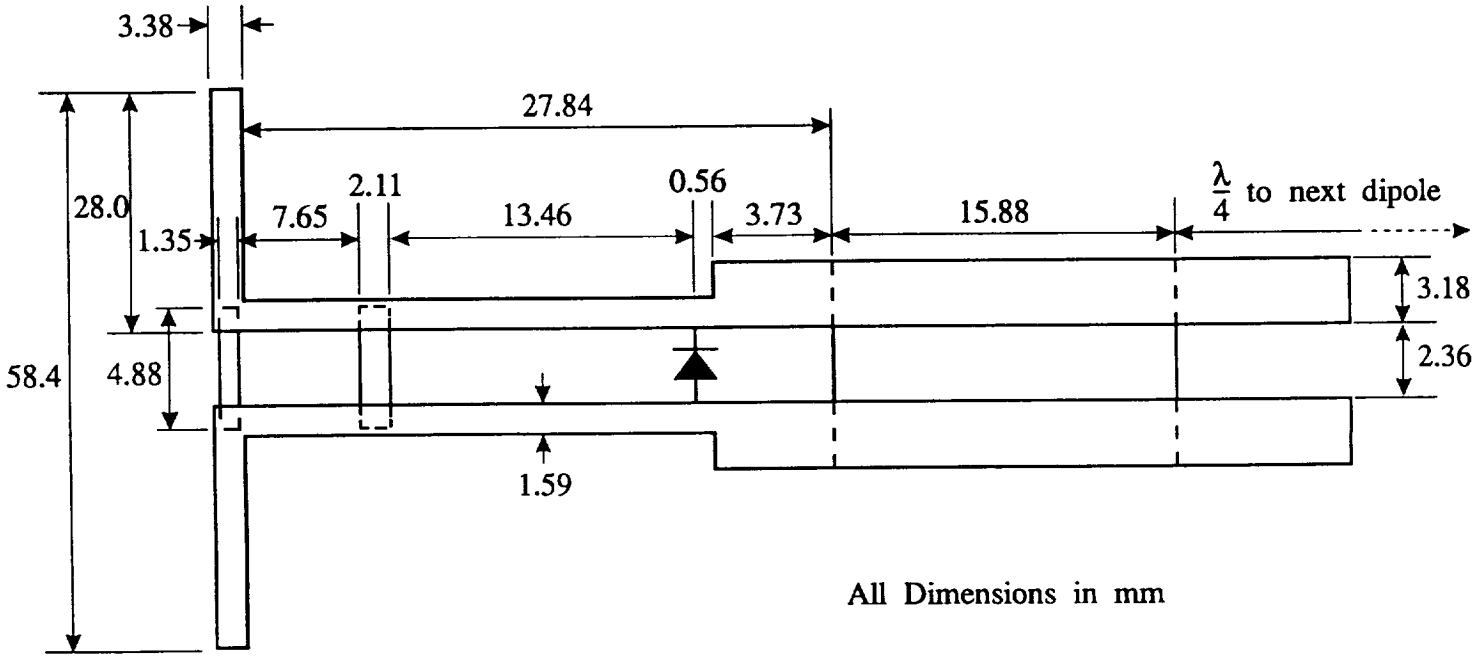


Figure 6. Physical rectenna layout and dimensions.

The dimensions of the coplanar stripline are based on the dielectric constant of the substrate and the desired impedance. Because the Kapton film is electrically thin ($<< \lambda$) at 2.45 GHz, a dielectric constant of 1.0 is used. To obtain the 270 Ω transmission line, the

strip width (W) is 1.59 mm and the separation gap (S) is 2.36 mm. The equations to calculate the characteristic impedance of coplanar stripline are given below [8]:

$$k = \frac{S}{S + 2W} \tag{15}$$

$$k' = \sqrt{1 - k^2} \tag{16}$$

$$\frac{K(k)}{K'(k)} = \frac{\pi}{\ln\left(2\,\frac{1 + \sqrt{k'}}{1 - \sqrt{k'}}\right)} \quad \text{for } 0 \le k \le 0.707 \tag{17}$$

$$Z_o = \frac{120\,\pi}{\sqrt{\frac{\varepsilon_r + 1}{2}}}\frac{K(k)}{K'(k)} \quad \text{(ohm)} \tag{18}$$

The diode is the most important component for efficiently converting microwave power into DC power because it is the main source of loss [7]. Plated heat sink Schottky barrier diodes with a GaAs semiconductor have proven to be the best device for this conversion process. The circuit model and parameter values of the Schottky barrier diode are shown in Figure 7. The diode parameters are the package inductance $L_p$, the series resistance $R_s$, the package capacitance $C_p$ , the junction capacitance $C_j$, and the junction resistance $R_j$ [9].

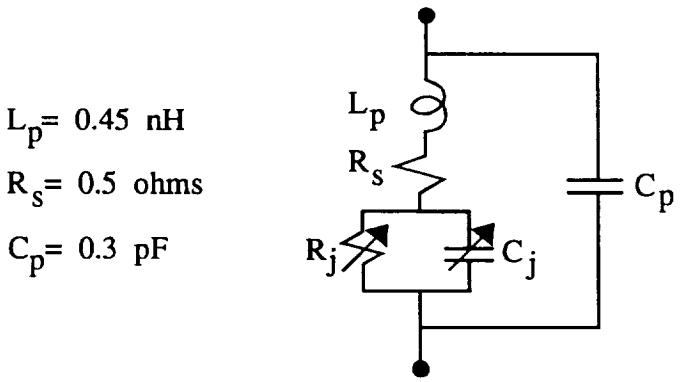


Figure 7. Schottky barrier diode model and parameters.

The zero-bias junction capacitance $C_{jo}$ is typically 3.5 to 3.8 pF.

The series resistance $R_S$ is important in determining the efficiency of the diode. As seen in Figure 7, this value is low. In the conduction portion of the rectification cycle the DC current flows through it, while on the non-conducting portion the charging current flows through the junction capacitance. The value of $R_S$ depends upon the semiconductor material used, the doping density of the epitaxial layer, the thickness of the epitaxial layer, and the area of the Schottky barrier junction.

Another important parameter is the breakdown voltage of the diode at which the diode starts to conduct in reverse bias. The breakdown voltage ($V_{br}$) is typically 2.5 times the DC output voltage of the rectifier. The parameter $V_{br}$ determines the doping density of the epitaxial layer, the zero-bias junction capacitance $C_{jo}$, and its minimum thickness, and thus, in combination with the area of the junction, the series resistance $R_S$ of the diode. Maximum output power is limited by the breakdown voltage of the diode. Typical breakdown voltages range from -55 V to -70 V. Figures 8 and 9 show a typical IV trace of this type of high power diode.

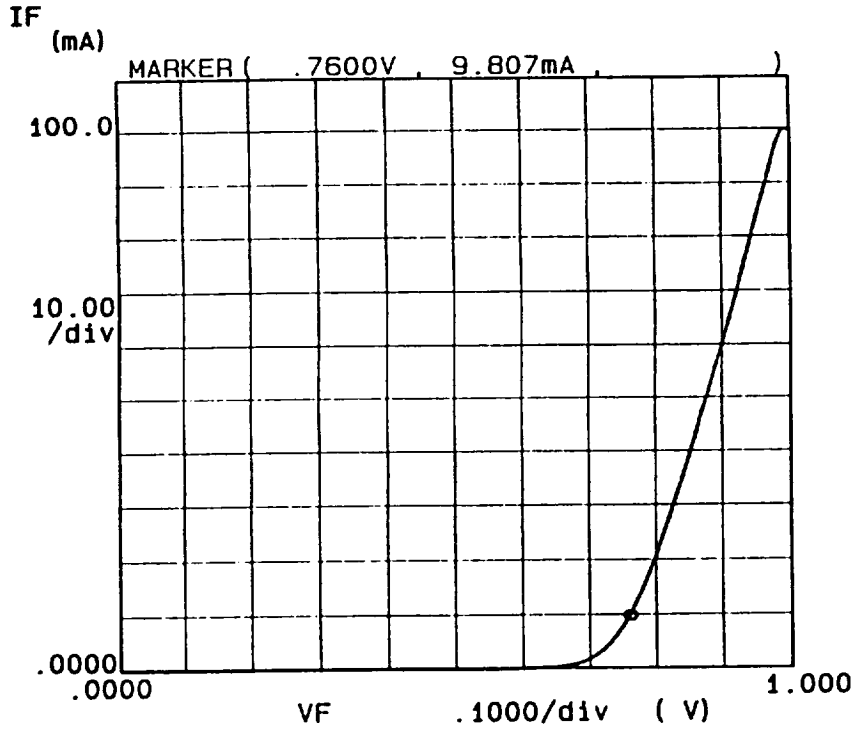


Figure 8. Typical IV trace of forward biased Schottky barrier diode.

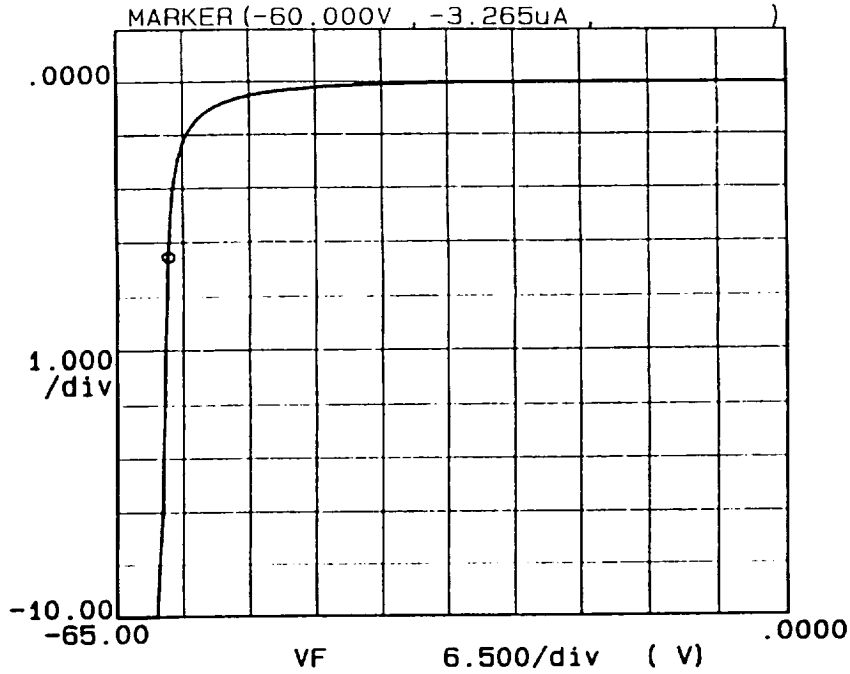


Figure 9. Typical IV trace of reversed biased Schottky barrier diode.

These diodes are extremely efficient in converting the microwave power into DC power and are very durable. They can convert the power at input levels of 10 W per diode. The physical construction of the diode is shown in Figure 10 [6]. An important aspect of this construction is the 1 mil gold wire connecting the top of the diode to the GaAs chip. Due to the wires small diameter, it will burn in half if too much current flows through the diode. In an array of rectenna elements, the wire protects the array by preventing the current from shorting through one diode.

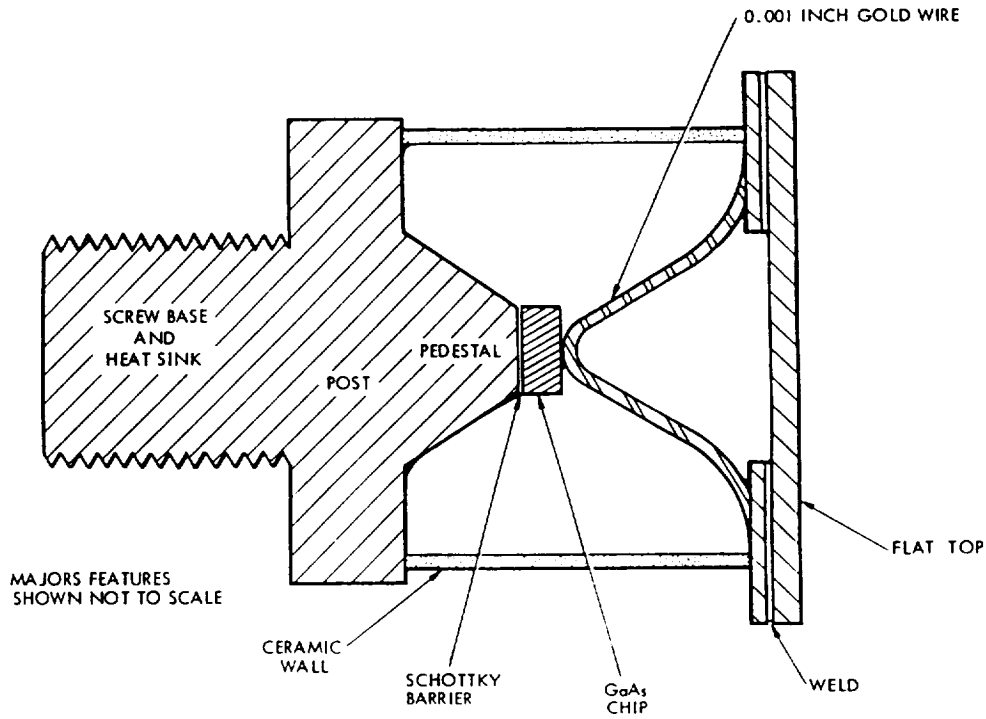


Figure 10. Cross section view of GaAs Schottky barrier diode.

The large signal model of the diode is represented by a resistor and capacitor in series. For coplanar stripline, it is convenient to convert the series elements into parallel elements as shown in Figure 11.

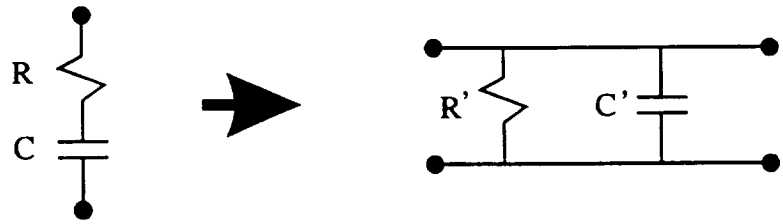


Figure 11. Series and parallel circuit configurations of large signal diode.

The equations to convert the resistor and capacitor from series form into parallel form are given as

$$R' = R + \frac{X^2}{R} \quad \text{where } X = \frac{1}{\omega C} \tag{19}$$

$$C' = \frac{C}{\frac{R^2}{X^2} + 1} \tag{20}$$

The efficiency of the rectenna is dependent on the DC load resistance. This implies that the diode input impedance is dependent on the DC load. For high conversion efficiencies, the DC load resistance is typically 1.3 to 1.4 times the diode input impedance [3]. The characteristic impedance of the coplanar stripline is 270 Ω, therefore a load resistance value of 350 Ω to 380 Ω will produce a conversion efficiency around 85%. Figure 12 shows the efficiency of a single thin film rectenna element as a function of DC load resistance and operating DC output power level [10].

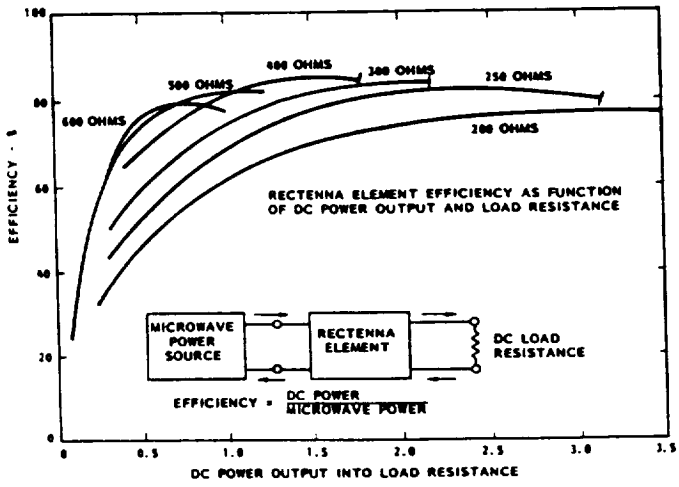


Figure 12. Single rectenna element efficiency as a function of DC load resistance.

Using Figure 12, it is possible to design a rectenna based on the DC load and output power. The characteristic impedance of the coplanar stripline is then determined from the ratio between the DC load to diode input impedance. Thus, Figure 12 can be used to match the diode input impedance to the characteristic impedance of the transmission line.

The dipole input impedance, diode input impedance, and DC load are all related. Efficient rectenna design cannot take place without understanding the relationship between these components. Efficient rectenna design also depends on the accurate prediction of the incident power density. The breakdown voltage of the diode is determined by this factor. The diode performs the highest conversion efficiency when the level of the incident power approaches the breakdown voltage of the diode.

The last circuit component, but equally important, is the large DC pass capacitor placed after the diode. This capacitor performs two vital tasks: 1) tunes the diode and 2) electrically shorts the microwave energy. The separation between this capacitor and the diode is critical for resonating the parasitic capacitance on the diode. In other words, the length of coplanar stripline between this capacitor and diode controls the inductance to resonate with the diode capacitance given in equation (20). The parasitic capacitance is composed of the diode package capacitance, effective junction capacitance, and mismatches between the diode and dipole. The capacitor is usually greater than 10 pF and its area is limited by spacing of the dipole antennas. A quarter-wavelength DC bus separates the end of the capacitor to the feed of the adjacent dipole. Since the capacitor acts as a microwave short circuit, the $\lambda/4$ spacing further isolates the rectenna elements by creating an open circuit at the adjacent dipole feed point.

The spacing between the dipole antennas is 0.635 $\lambda$. The elements are connected in rows of parallel rectennas, and for large arrays, the rows are connected in series. Even though each rectenna element is basically isolated from each other electrically, the input impedance of the dipole will change when placed in a large array. The surface waves which occur on top of a large array of rectenna elements affects the dipole input impedance. This aspect is one of the phased array effects of the rectenna.

Another phased array effect is the radiation of harmonics produced by the diode. As stated previously, the radiation pattern produced by the rectenna array at the operating frequency resembles a single element. However, the patterns created by the harmonics do resemble a phased array. Figure 13 shows the second harmonic (4.9 GHz) radiation pattern produced by a a 4 x 5 rectenna array. The pattern was measured by recording the radiation level when rotating around the rectenna while the rectenna was illuminated at normal incidence by the power source. Normal incidence is marked at ninety degrees which is the broadside direction of the array. As seen from the figure, peaks and nulls are detected as a normal phased array.

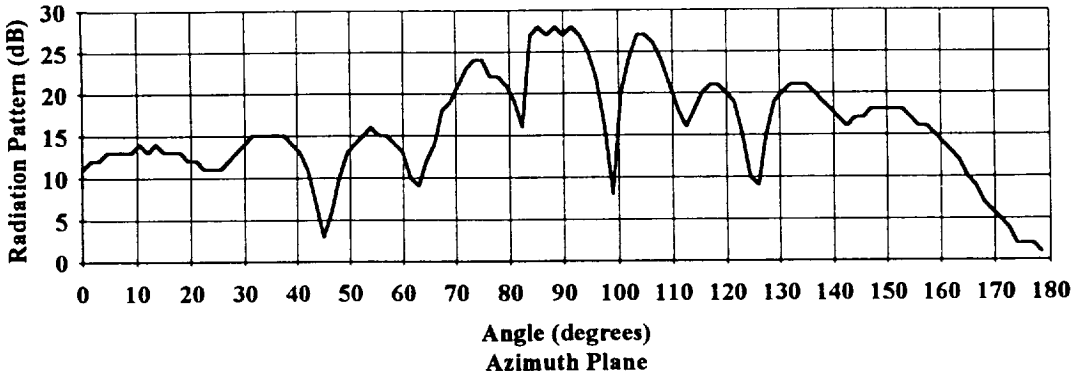


Figure 13. Second harmonic radiation produced by a 4 x 5 element rectenna array.

**METS Rectenna:**

The METS rectenna is an unique application of the rectenna. In the METS experiment, the rectenna is acting as a microwave power detector. The rectenna is located on the daughter payload section and is released from the mother section during the experiment. The microwave power beam from the mother section will transmit in directions away from the daughter section. Any microwave power located near the daughter section will be detected and sent to the instrumentation package as a 0 to 5 V signal. Voltage limiters (zener diodes) were placed across the DC load to protect the instrumentation. Due to the close proximity of the daughter section to the transmitter, the received microwave power may be produced by the main beam or as sidelobes. Figure 14 shows the top view of the METS spacecraft with the American and Japanese rectennas unfolded. The arrows located on the microwave power transmitter indicate the transmit polarization.

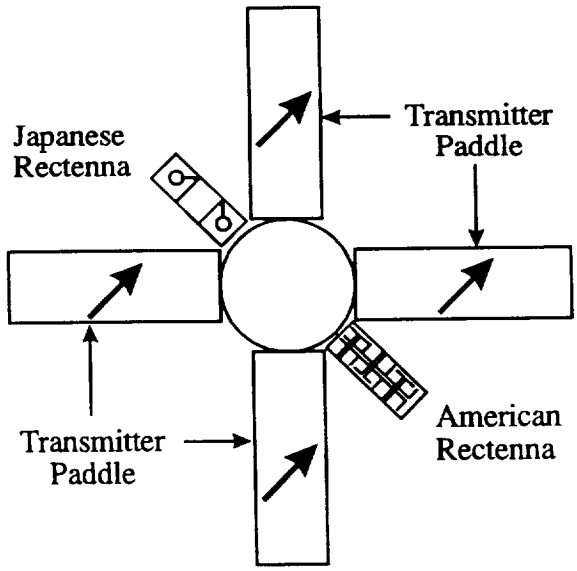


Figure 14. Top view of METS mother and daughter spacecraft sections.

The operating frequency of the power transmitter is 2.411 GHz. The METS rectenna is designed for 2.45 GHz but there is minimal, if any, reduction in performance.

The packaging of the METS rectenna was also unique due to the size constraints and the performance. The dimensions specified the rectenna package to be 27 cm long, 10 cm wide, and 1.6 cm tall. The rectenna circuit is etched on the thin film Kapton as discussed in the theory section, and the single element dimensions are shown in Figure 6.

The spacing between the rectenna plane and the reflecting plane is normally 2 to 2.5 cm. This spacing was reduced to 1.1 cm as mandated by the package contents. The reduction of this separation causes an impedance mismatch between free space and the rectenna dipoles input impedance (120 $\Omega$). Theoretical calculations indicate the dipole input impedance to be approximately 25 $\Omega$ when spaced 0.11 $\lambda$ above a reflecting plane [11]. However, the transmitted power from the mother section is predicted to be 800 W, and this impedance mismatch will help to protect the rectenna circuitry from large power densities. Because rectenna efficiency will not be considered, the impedance mismatch works for the rectenna.

After releasing from the mother section, the daughter section is expected to rotate off axis from the mother section. The rectenna described in the theory section is linearly polarized, and the transmitter on the mother section is also linearly polarized. To prevent the rectenna polarization from being misaligned from the transmitter polarization, a second rectenna layer was added. The second layer is 90° out of phase with the first rectenna layer to create dual polarization. This construction is similar to an existing single foreplane rectenna with dual polarization [12].

The rigorous forces and vibrations imposed on the rectenna during the rocket launch necessitated strong materials and construction. The shock during launch is predicted to be 40 g for 10 milliseconds. This force equates to a 140 g static load. The vibration is 3.06 mm (amplitude) for 10 to 35 Hz, 7.5 g for 35 to 400 Hz, and 15 g for 400 to 2,000 Hz. The material selected to house the rectenna was G10 fiberglass. The G10 block was cut by carbide milling tips to the specified dimensions and tapped for the screws to hold the reflecting plane. Holes for spring pins were also drilled between the screws. A lip overhang was milled into the top of the G10 frame to secure the contents.

Different layers of materials were placed in the package to hold and secure the rectenna layers. The top covering in the broadside direction of the rectenna was selected to be 5 mil Kapton. This Kapton layer was placed under the lip on the G10. An epoxy glue made by B.F. Goodrich was used to bond the Kapton to the G10 lip. A 20 mil layer of Volara 6E foam was placed underneath the Kapton covering. Because the dielectric constants of the Kapton ( $\varepsilon_r = 3.8$) and Volara foam ($\varepsilon_r = 1.08$) are low and their thickness is much less than the wavelength at 2.411 GHz, these materials are basically RF transparent and do not effect the rectenna's performance. The first rectenna layer was composed of separate rectenna elements. A second Volara foam layer is placed between the rectenna layers to electrically isolate them and to securely hold them. Rigid ROHACELL foam made by

Rohm is used to separate the reflecting plane from the rectenna layers. ROHACELL grade 71 has a low dielectric constant ($\varepsilon_r$ = 1.08 at 2.0 GHz) and a low loss tangent (0.0003). This product is ideal for this application due to its rigidity, low dielectric constant, and ease in milling to the correct height. A 60 mil aluminum reflecting plane was then secured to the G10 frame by screws. Eighteen 4-40 size screws, six 8-32 screws (grade 8), and 12 spring pins connected the reflecting plane to the G10 frame. The screws were bonded to the frame by Loc-Tite 410. Figure 15 shows the contents of the rectenna package and figures 16 and 17 show the dimensions of the G10 frame.

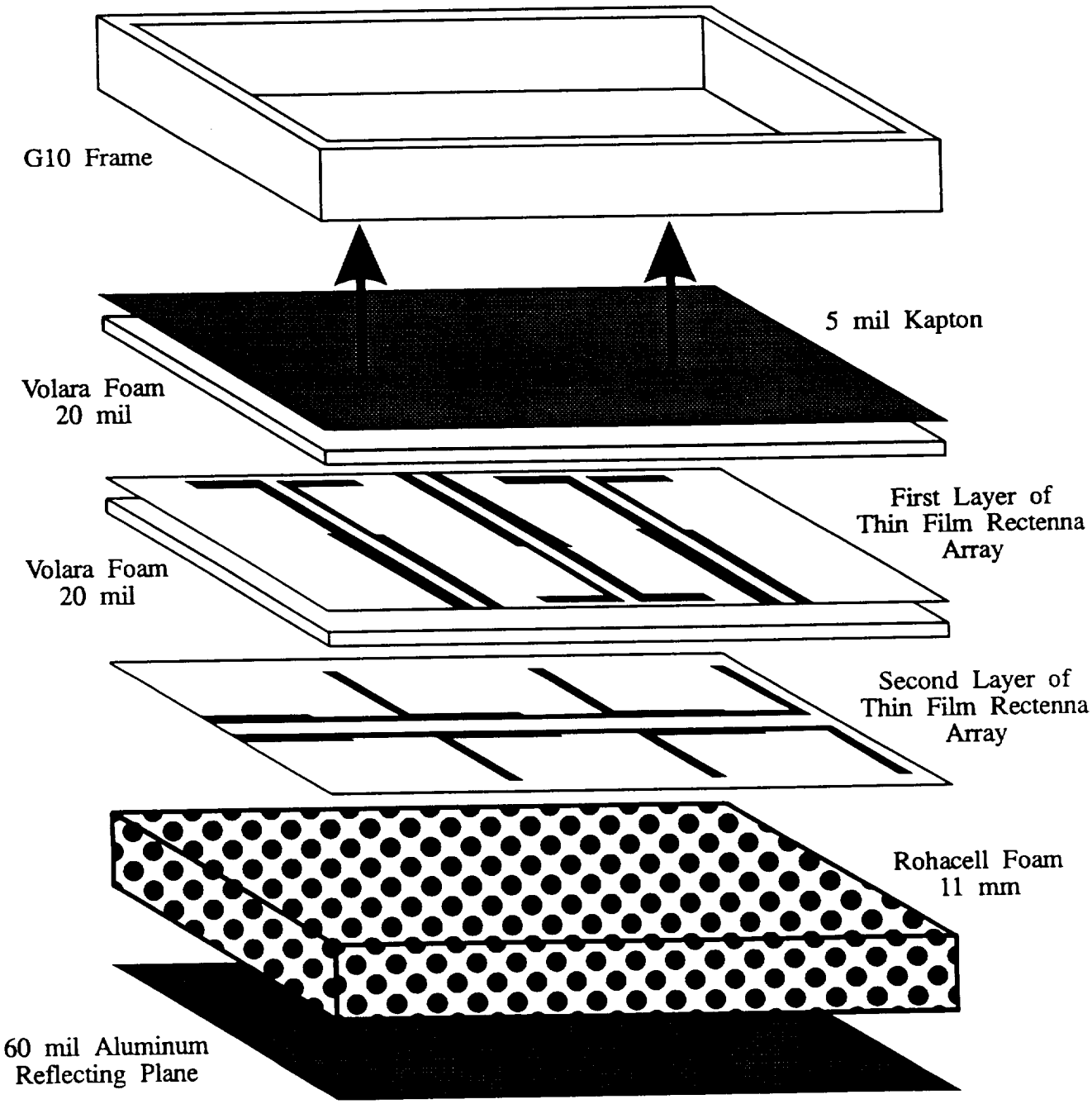


Figure 15. Package contents of METS rectenna.

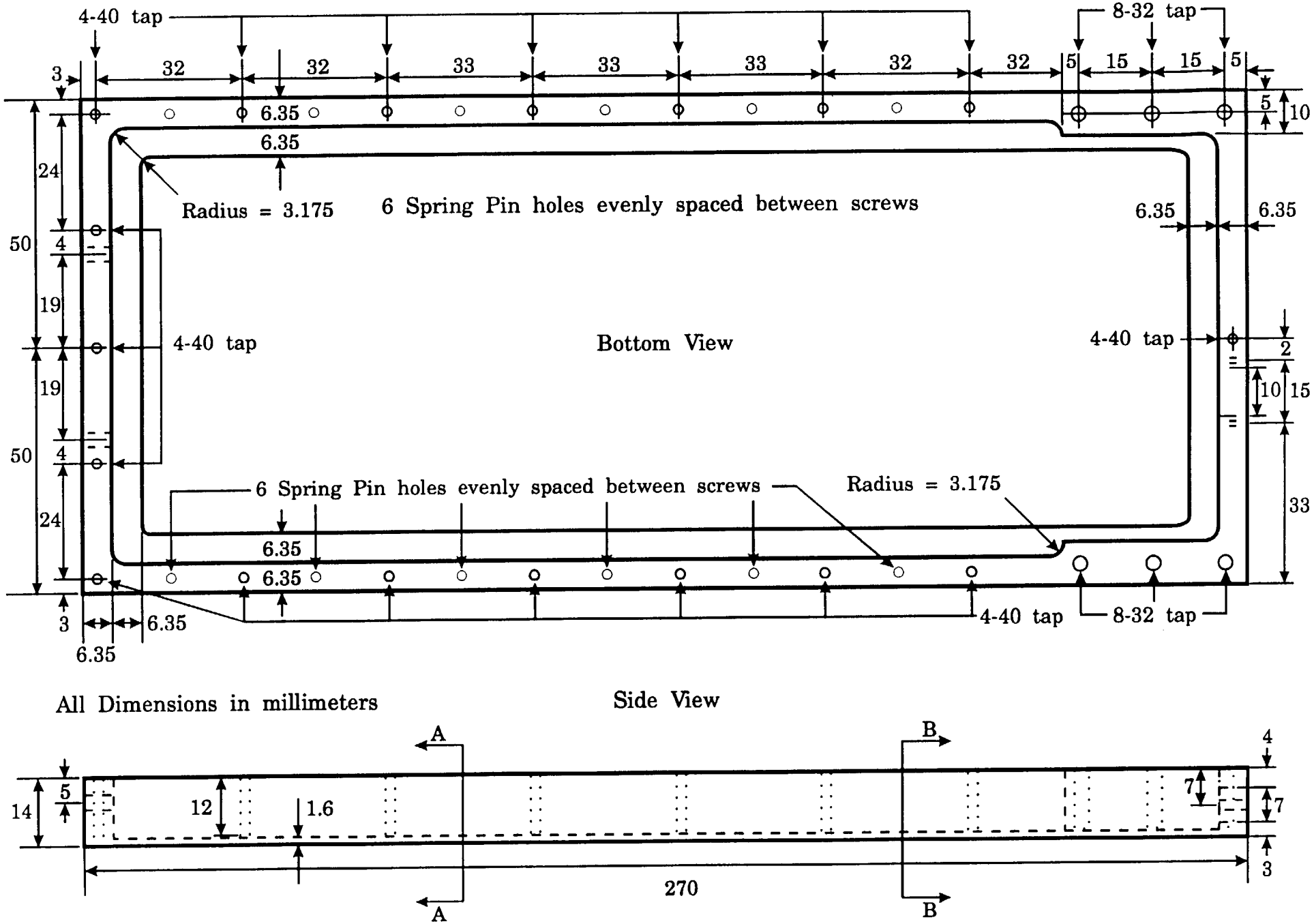


Figure 16. Bottom and side views of G10 frame for METS rectenna.

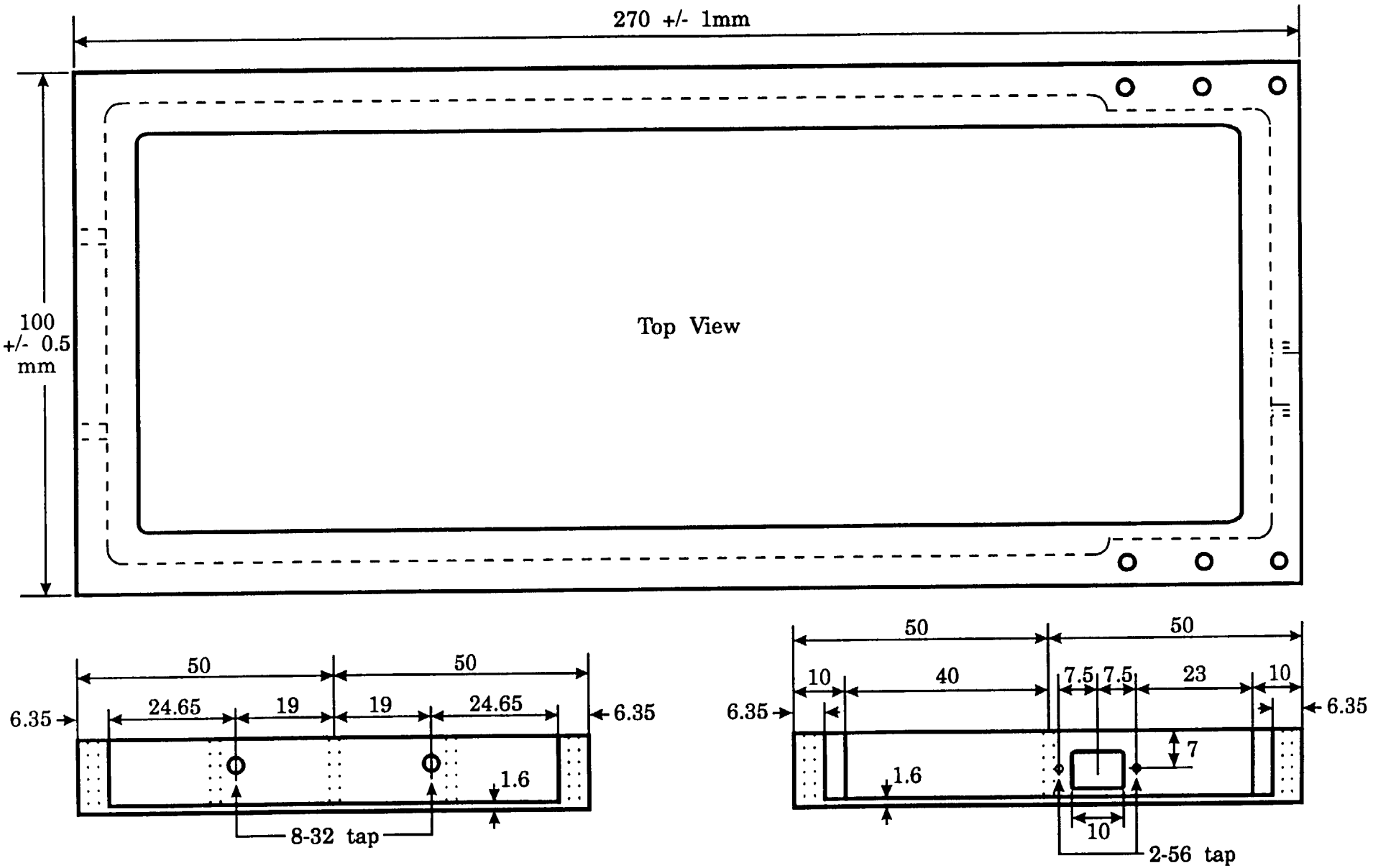


Figure 17. Top and section views of G10 Frame for METS rectenna.

Six IMPATT GaAs diodes were ordered from M/A-COM, Inc. These surface mount diodes (model # M/A 46137 with $C_{jo}$ = 3.6 pF) are designed as microwave sources in the X-band. For the rectenna application, these Schottky barrier diodes are used in a reverse process. Instead of generating an oscillation from a DC source, the diodes convert microwave power into DC power in the S-band. The breakdown voltage of the diodes is 55 V. The requirements for an efficient rectenna diode as discussed in the theory section are met by these IMPATT diodes.

Due to excessive power densities on the METS rectenna, the heat dissipation from the diodes is an important issue. Copper strips of 20 mil thickness were glued to the DC bus lines on each rectenna element to act as heat sinks. The same epoxy glue used to bond the Kapton cover to the G10 frame was applied to bond the copper strips to the copper transmission lines. Figure 18 shows where the copper strips were applied.

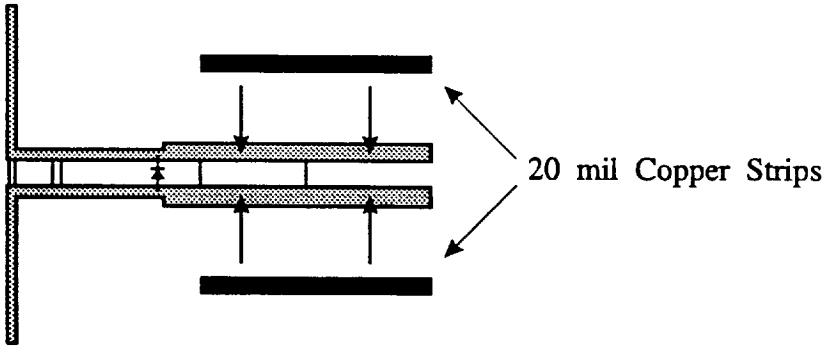


Figure 18. Placement of the copper strips on the rectenna elements.

The rectenna layers were positioned as shown in Figure 19. Due to the dimensional constraints of the rectenna package, the top layer of rectenna elements could not be located in the optimum positions. The elements were placed equally between the elements on the bottom layer.

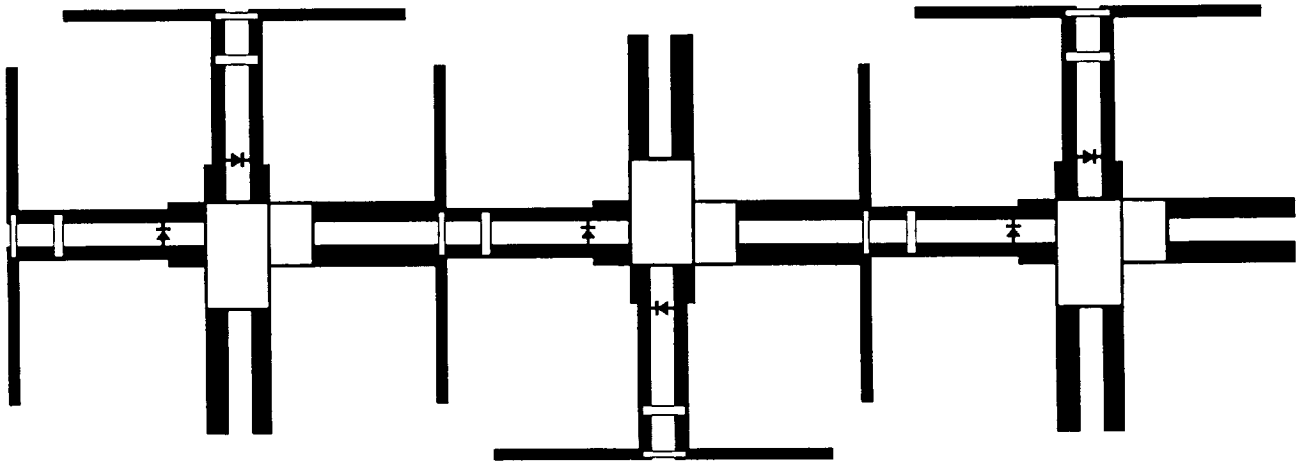

Figure 19. Stacked layers of rectenna elements in METS rectenna package.

The middle element of the top layer was reversed to isolate its dipole from the dipoles of the outside elements. Experimental evidence proved the output voltage was increased by reversing the middle element. Thus, the rectenna's performance was improved as a detector. Figure 20 shows the dimensions of the top layer of rectenna elements. The DC pass capacitor, represented by the large white patch, was located directly on top of the bottom layer's DC pass capacitor. This placement minimized field interference on the transmission lines between the two layers. The top layer rectenna elements are connected in parallel by wires that run underneath the ROHACELL foam.

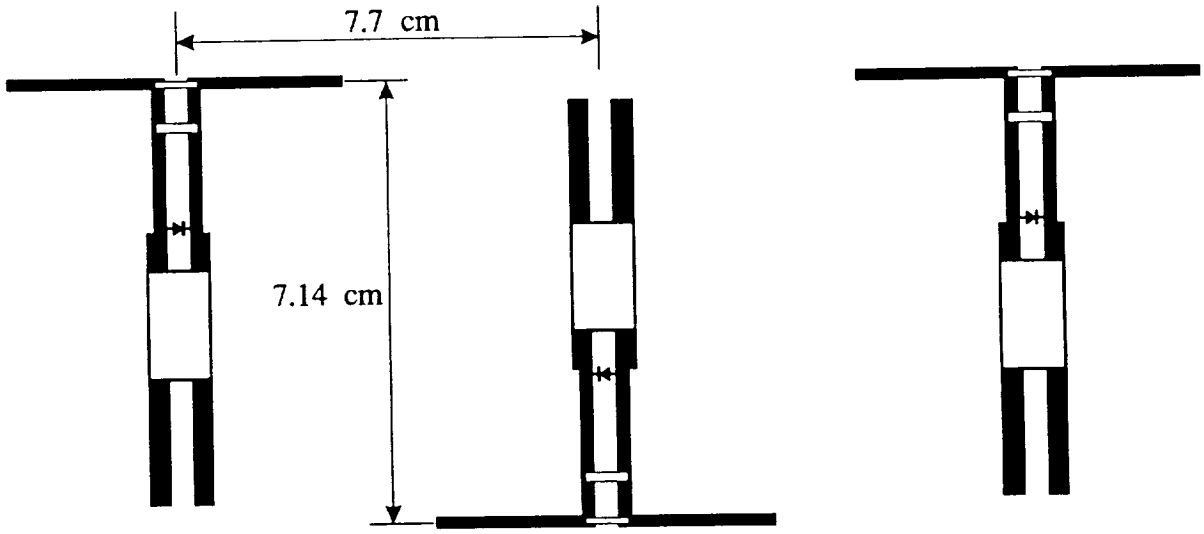


Figure 20. Spacing between top layer rectenna elements.

The DC power is collected by electrically insulated wires that connect the output of each array (top layer and bottom layer) to the DC resistive load. The DC load is capable of dissipating 25 W of DC power by zener diodes. The DC load package is shown in Figure 21.

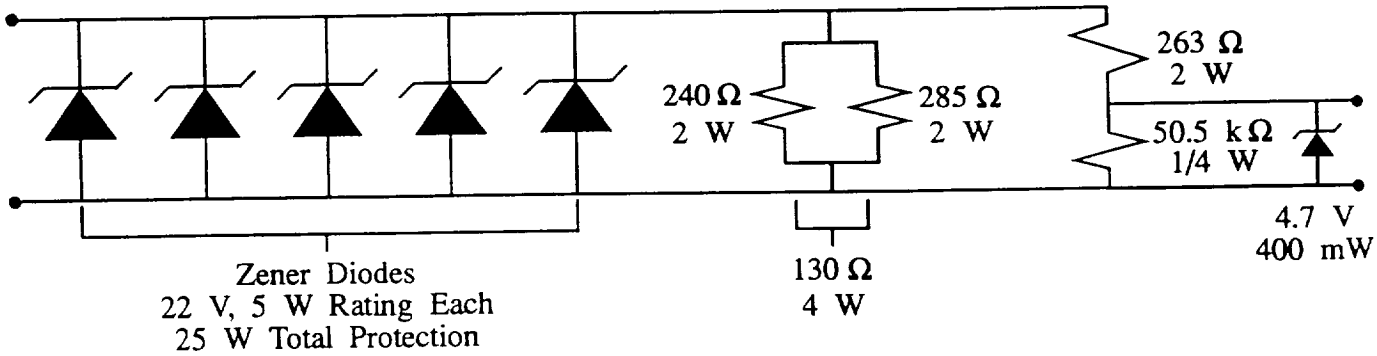


Figure 21. DC load and zener diodes.

The resistive load as seen by the rectenna arrays is 130 Ω. Because the three rectenna elements in each layer are connected in parallel, each element has a 390 Ω load. This load was targeted for the METS rectenna based on the efficiency curve in Figure 12. The rectenna will perform well as a detector with this load. The maximum power the 130 Ω load will receive is 3.72 W, so the total rating of the two resistors in parallel is 4 W. The power rating on each of the 22 V zener diodes is 5 W. The power rating with five of these diodes in parallel is 25 W. Based on the separation distance between the mother and daughter sections during the experiment, transmitted power, and estimated sidelobe power, a rating of 25 W will provide adequate protection to the rectenna circuit. The 22 V level of the zener diodes is based on the breakdown voltage (55 V) of the rectenna diodes.

Two different types of resistive loads were tried. A 5 W wire wound resistor was first used. This type of resistor has capacitive and inductive elements which interact with the microwave power beam. A spurious signal a 320 MHz was generated during the rectenna testing. After switching to a carbon resistive load and shorting of the wire leads between the rectenna and the load, the spurious signal disappeared. Figures 22, 23, and 24 show the 2 kHz to 10 GHz spectrum when the METS rectenna was operating. The harmonics produced by the rectenna diode are shown in figures 23 and 24.

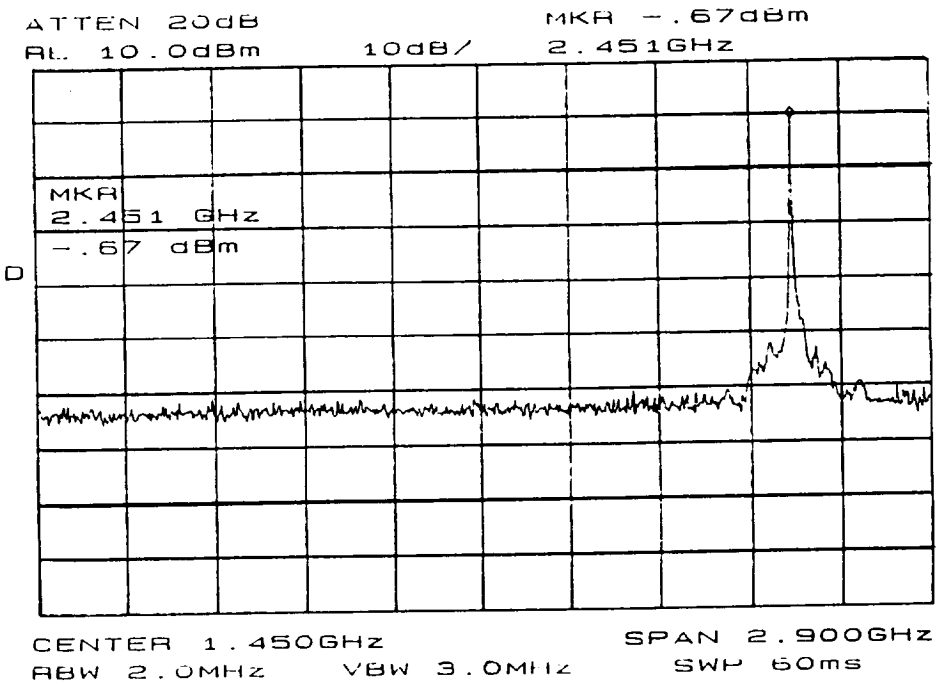


Figure 22. Measured spectrum when operating the METS rectenna, 2 kHz to 2.9 GHz.

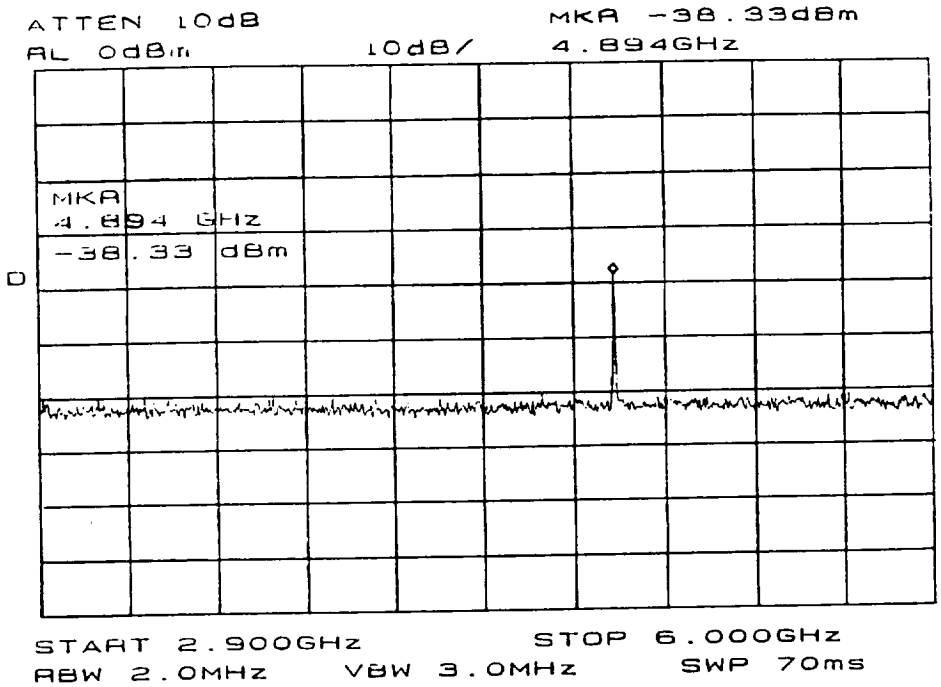


Figure 23. Measured spectrum when operating the METS rectenna, 2.9 to 6 GHz.

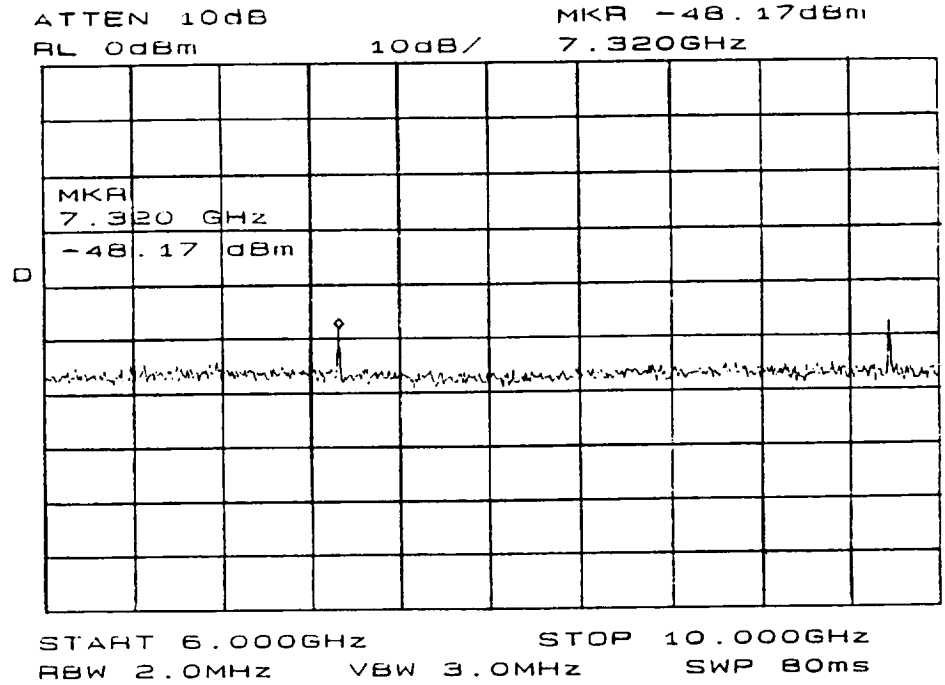


Figure 24. Measured spectrum when operating the METS rectenna, 6 to 10 GHz.

To prevent the maximum output voltage from exceeding 5 V, a voltage divider circuit was designed. The maximum current through the 263 Ω resistor is 66 mA. Thus, the maximum power delivered to this resistor is 1.14 W and the 2 W rating will protect the resistor. Using the same maximum current, the maximum power seen by the output 4.7 V zener diode is 309 mW. The 400 mW rating on this output diode will also handle this power level.

The testing of the METS rectenna involved many configurations and orientations. All tests were performed with a separation distance of 35 inches (89 cm) between the transmitter and the rectenna. The power density at the rectenna was calculated by the Friis equation as

$$P_{density} = \frac{P_{out} G_{trans}}{4 \pi R^2} \tag{21}$$

where a horn antenna was used as the transmitter that had a gain of 9.63 dB. The output power was measured by use of a voltmeter across a 130 Ω resistor.

Figure 25 shows the results of the top layer rectenna elements with the electric field from the transmitter polarized with the dipole antennas. The elements were tested without the G10 frame. As shown, the performance increases when the middle rectenna element is reversed. The reason for the increased performance is the improved isolation between the dipoles. The capacitive fringing that occurred between the dipole ends had reduced the dipole efficiency. Therefore, the middle element was reversed for all following results.

Figure 26 shows the output voltage of both top layer and bottom layer rectenna arrays versus power density. The G10 frame was not used for these results either. As seen, there is little difference between the polarizations.

Figures 27, 28 and 29 show the results of the rectenna orientation to the polarization of the transmitted electric field with and without the G10 frame. As seen from the progression of the rotation, the effect of the G10 frame becomes prominent. The dielectric constant of the G10 is 4.8. Because a 1.6 mm lip of the G10 extends towards the dipoles on the top layer, the G10 influence greatly reduces the dipole performance. There exists another reduction in performance due to the reaction of the top layer rectenna with the bottom layer rectenna as seen when comparing the results of Figure 27 without the frame to Figure 25. However, the reduction in performance due to the frame and to the interaction between the layers helps to protect the rectenna circuit from high power densities.

Figure 30 shows the output voltage when the rectenna is rotated in a clockwise direction. Instead of a relatively flat line as would be expected from a dual polarized rectenna, the voltage output is reduced as the rectenna rotates towards the polarization of the top layer rectenna elements. This figure is an extension of figures 27, 28, and 29.

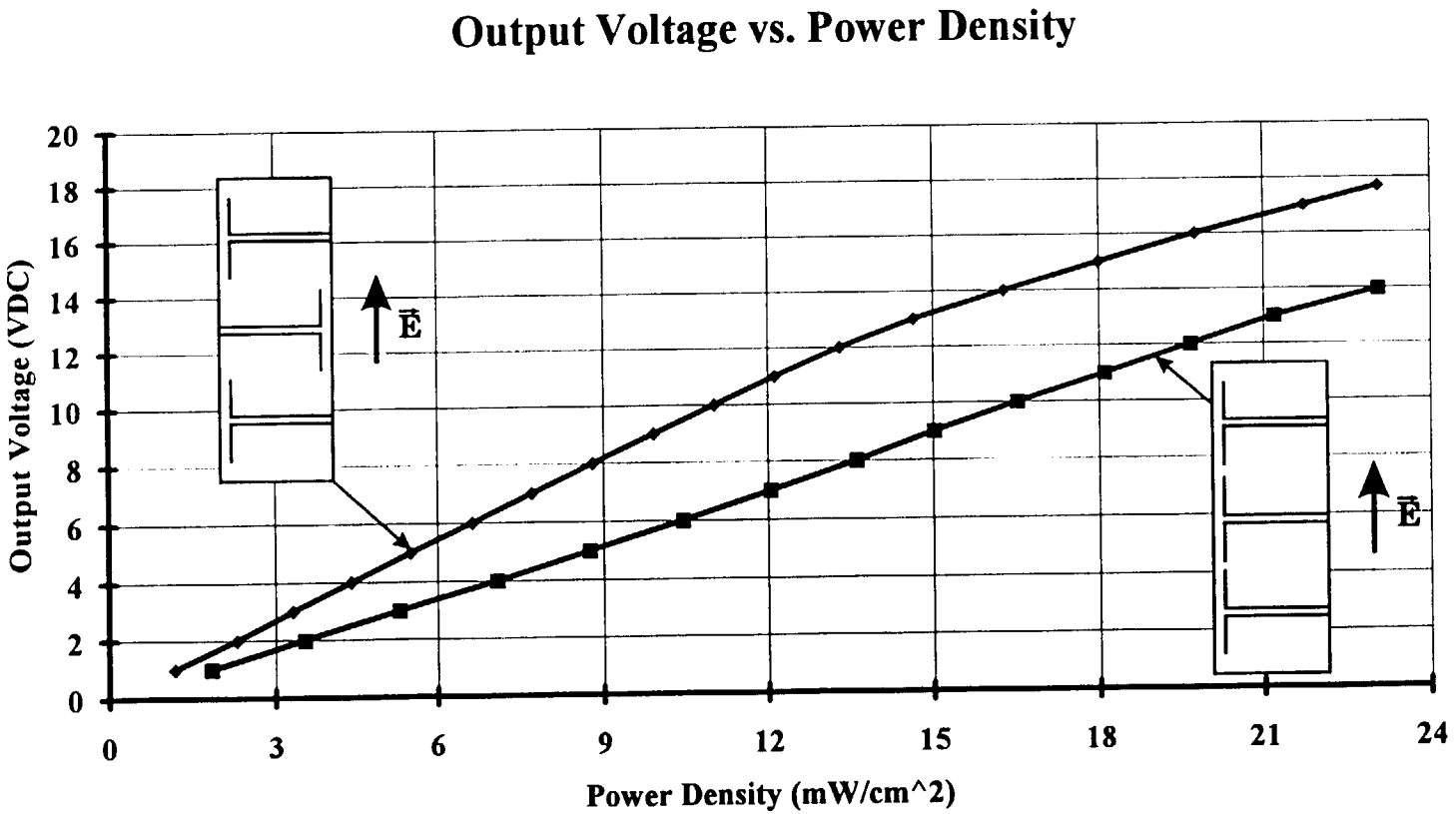


Figure 25. Performance comparison between reversed middle element and aligned middle element.

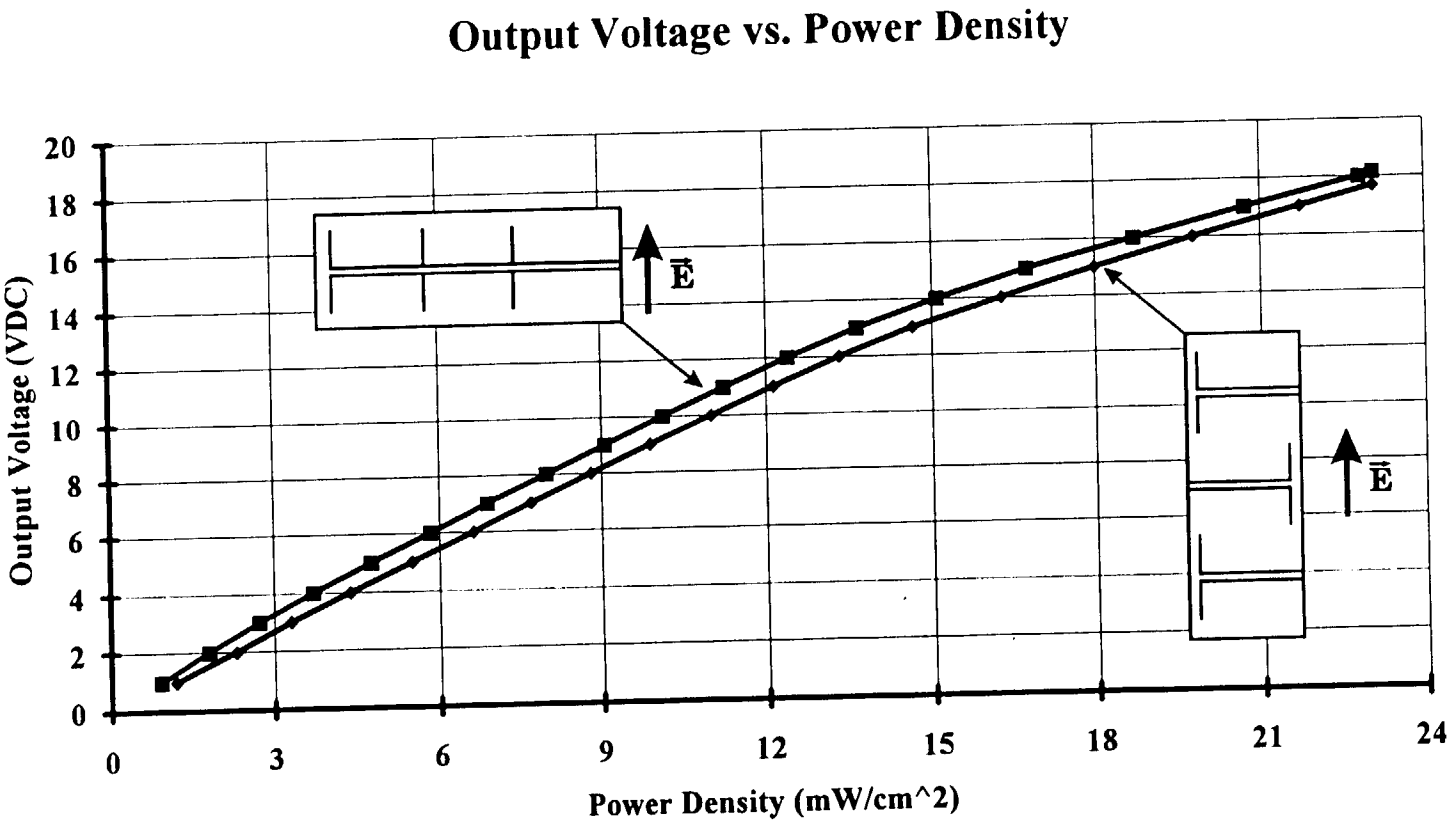


Figure 26. Performance comparison between the top and bottom rectenna layers without the G10 frame.

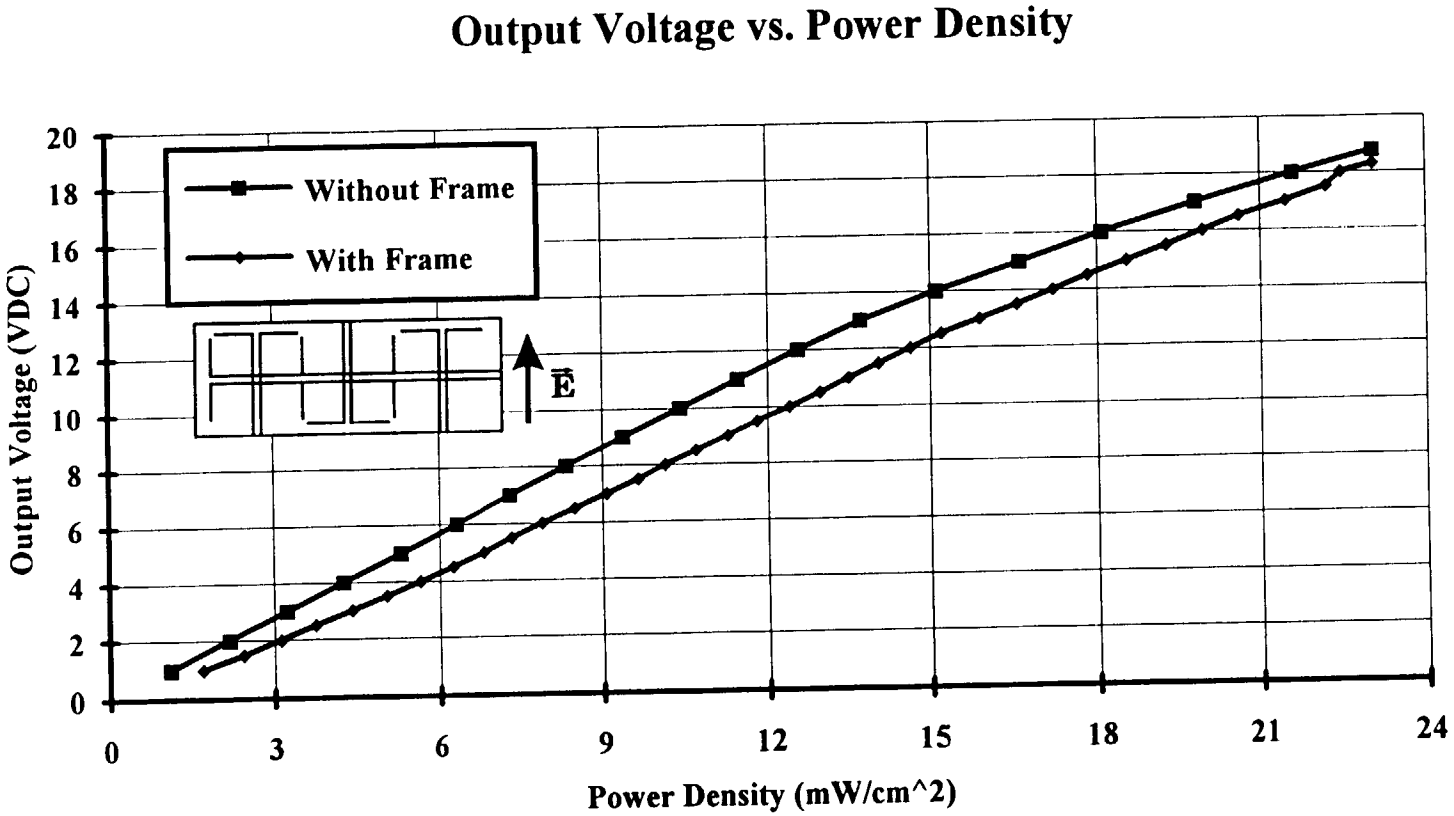


Figure 27. Performance comparison of bottom layer rectenna with and without the G10 frame.

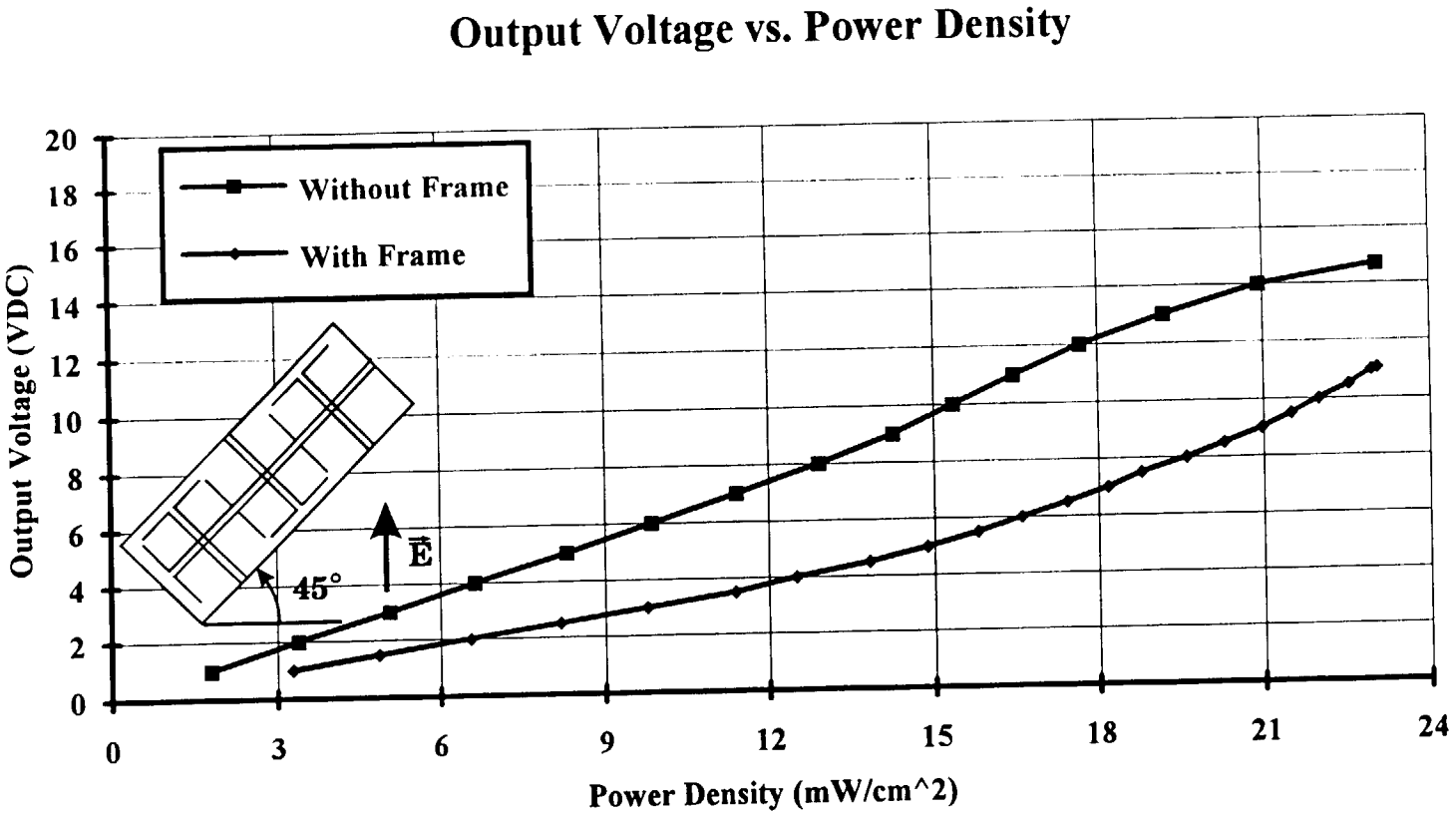


Figure 28. Performance comparison of rotated METS rectenna with and without the G10 frame.

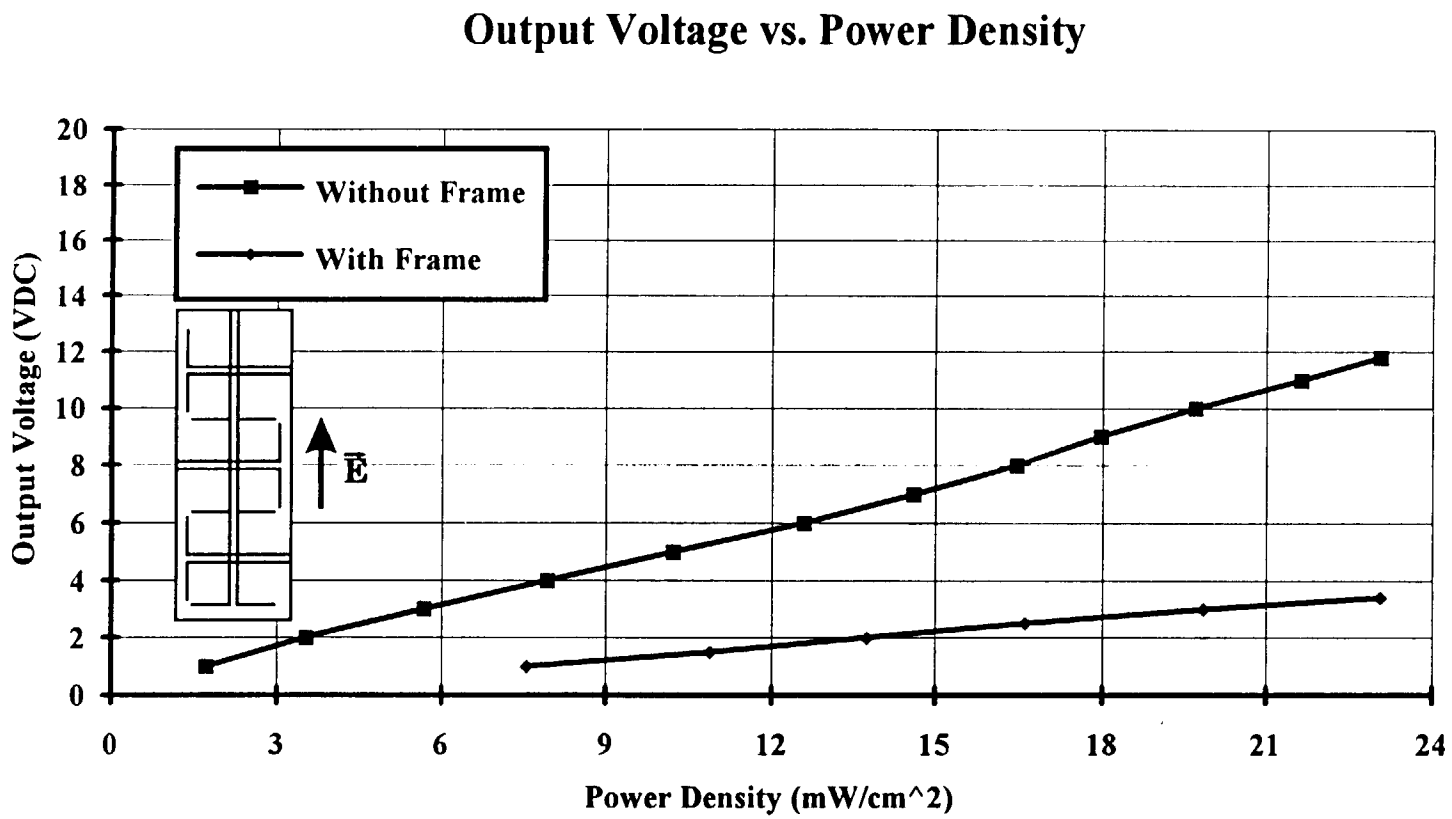


Figure 29. Performance comparison of top layer rectenna with and without the G10 frame.

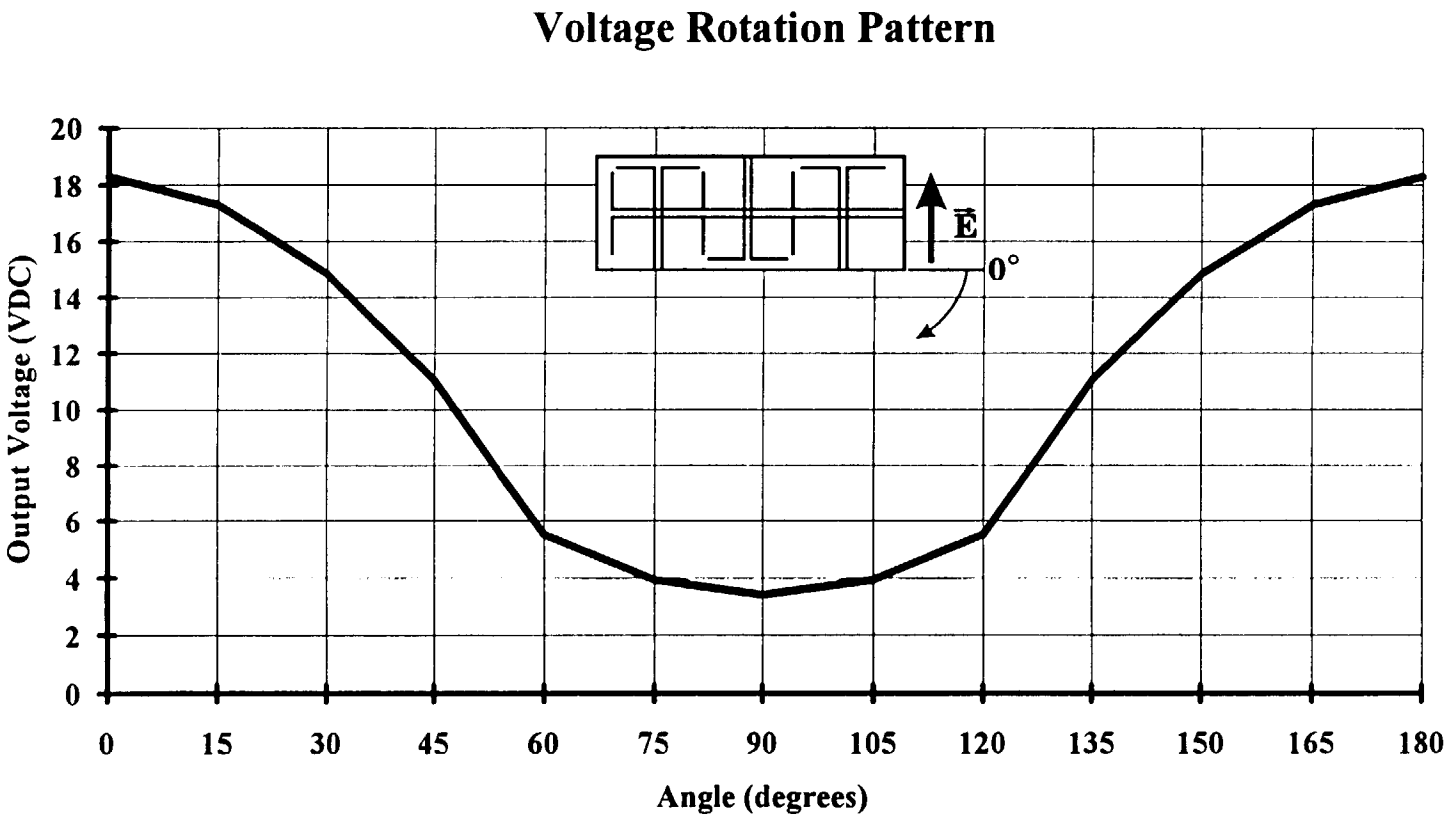


Figure 30. Output DC voltage versus rotation of the METS rectenna with the G10 frame.

Although the rectenna conversion efficiency is not a concern of the METS experiment, a test of this package was performed. Figure 31 shows the rectenna efficiency as the rectenna is rotated. The efficiency was calculated by use of the Friis equation as

$$\eta = \frac{\frac{V_{DC}^2}{R_{load}}}{\left(\frac{\lambda}{4\pi R}\right)^2 G_{trans} G_{rectenna} P_{trans}} \tag{22}$$

where the rectenna gain was calculated by

$$G_{rectenna} = \frac{4\pi}{\lambda^2} A_{effective} \tag{23}$$

The effective area of the rectenna was determined by using the value of 50 $cm^2$ per element. Thus 150 $cm^2$ was used for the effective area at all rotation angles. The same horn as mentioned earlier was used transmitting 250 W. The power density at the rectenna was 23.1 $mW/cm^2$. As seen from the figure, the efficiency drops dramatically from a peak of 75% to a low of 2.6%. This drop is due to the influence of the G10 frame on the top layer rectenna elements. Because a high power density may impinge on the rectenna, the inefficiency can serve as circuit protection.

Figures 32 and 33 show the output voltage pattern as the rectenna is rotated about their axis with respect to the particular polarization. These patterns emphasize an unique characteristic about rectennas as discussed in the theory section. Even though there are 3 elements in each array, there are no nulls on the output voltage. This type of antenna is quite different from normal phased arrays of uniform phasing and distribution which do have nulls and sidelobes.

A test was conducted on the DC load alone. A DC voltage source was connected to the load where the outputs from the rectenna would be located. The source was elevated to 23 VDC and the voltage from the 4.7 zener diode was recorded. The result is shown in Figure 34 which proved the effectiveness of the circuit design.

The final assembly, which included both layers of rectennas, the G10 frame, and the DC load circuit, was tested. The rectenna's detection performance at different orientations are shown in Figure 35. Although the curves diverge from each other as the polarization changes from the rectennas on the bottom layer to the rectennas on the top layer, the detection performance is good and the package can withstand large amounts of incident microwave power.

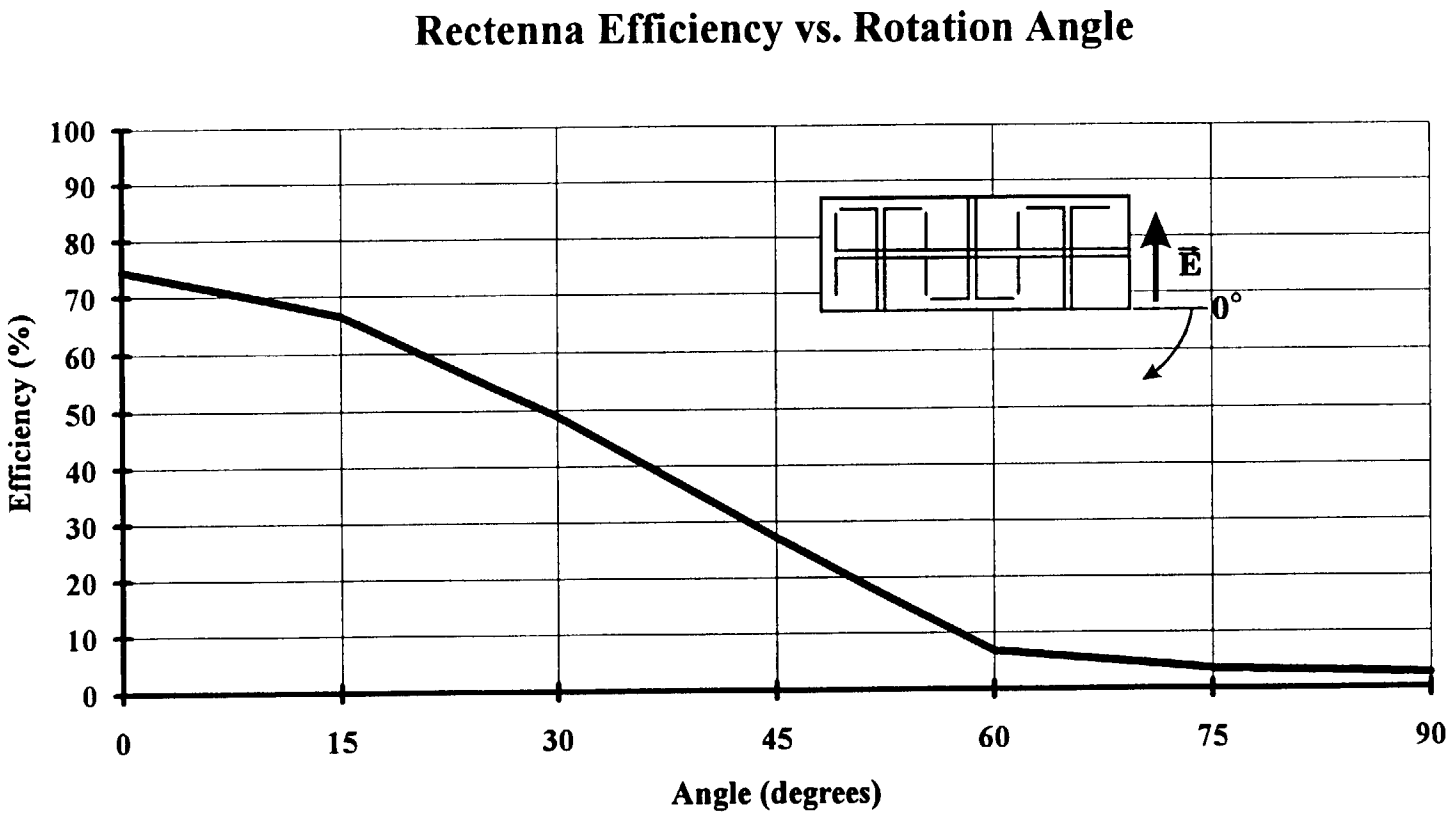


Figure 31. METS rectenna efficiency versus rotation angle with the G10 frame.

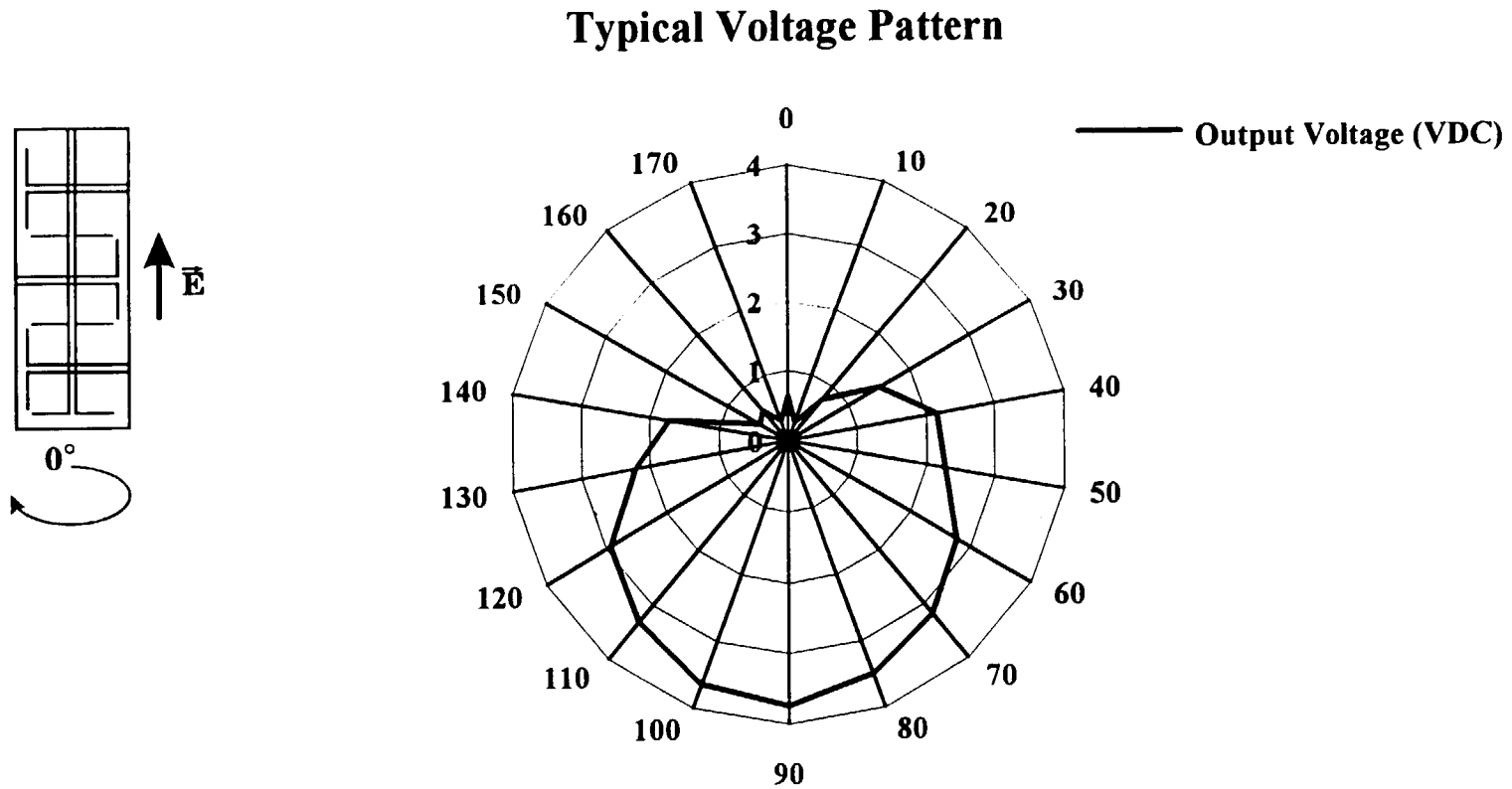


Figure 32. Outout voltage pattern of the top layer rectenna with the G10 frame.

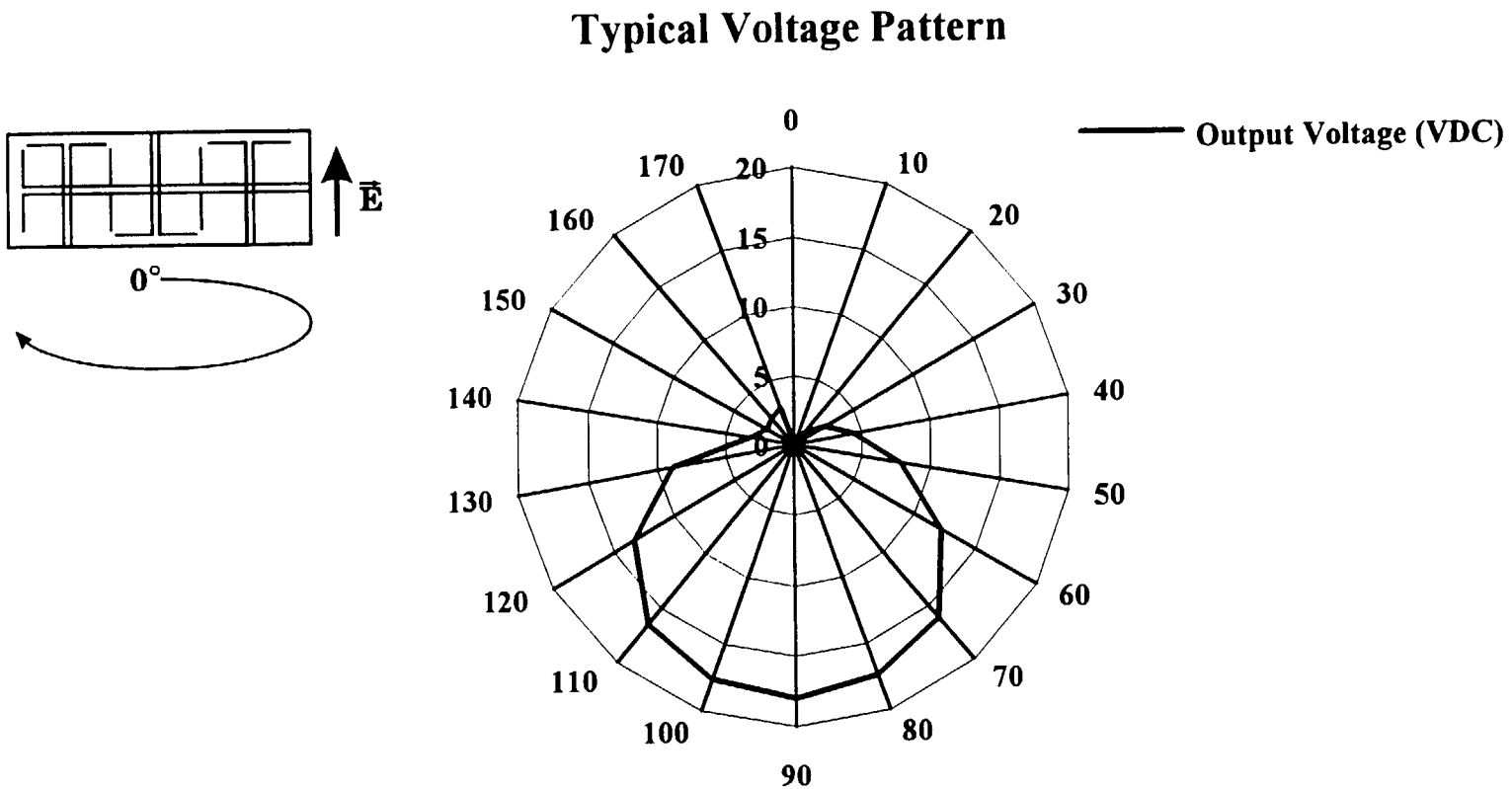


Figure 33. Outout voltage pattern of the bottom layer rectenna with the G10 frame.

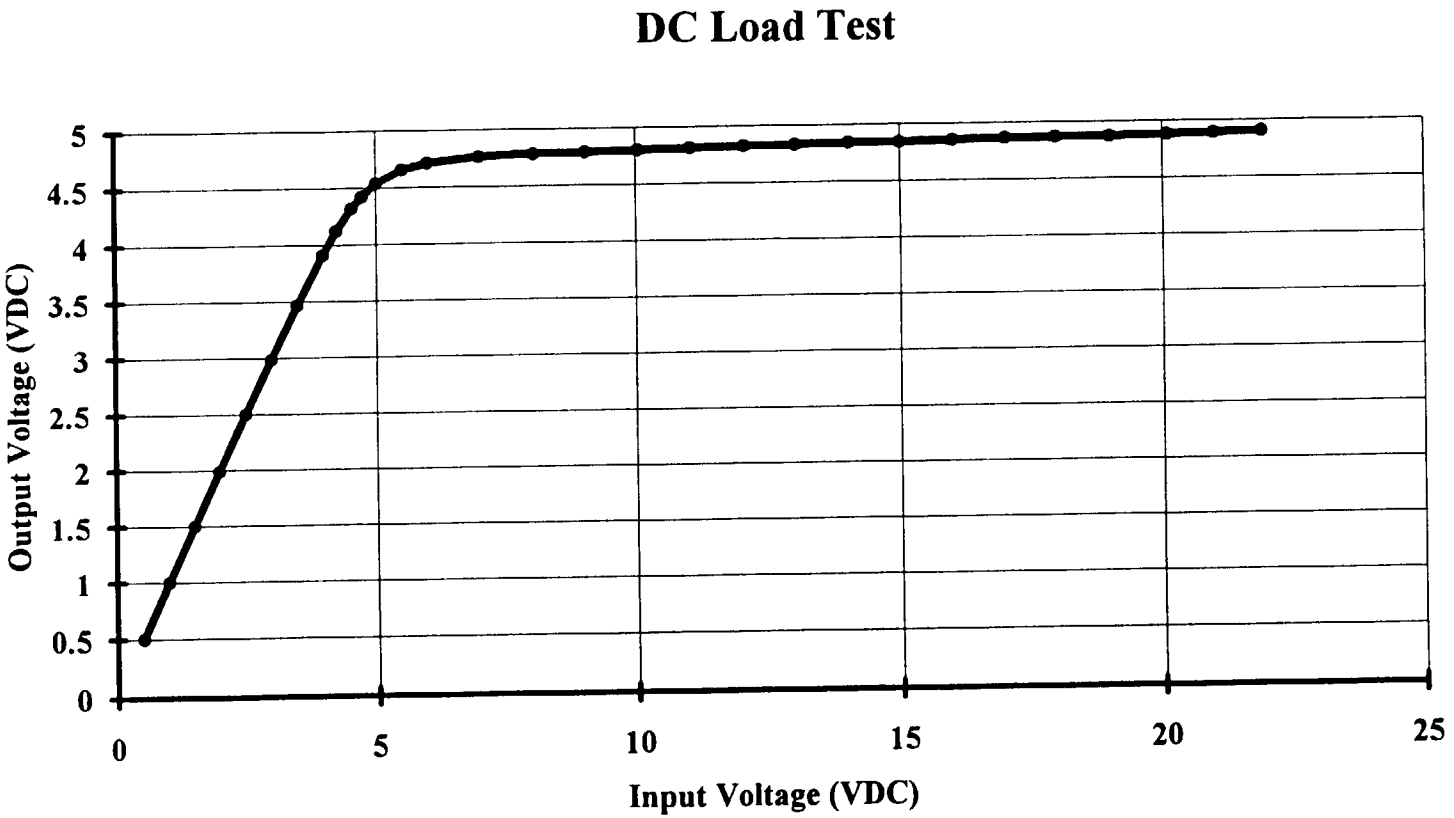


Figure 34. Output voltage versus input voltage on the METS rectenna DC load circuit.

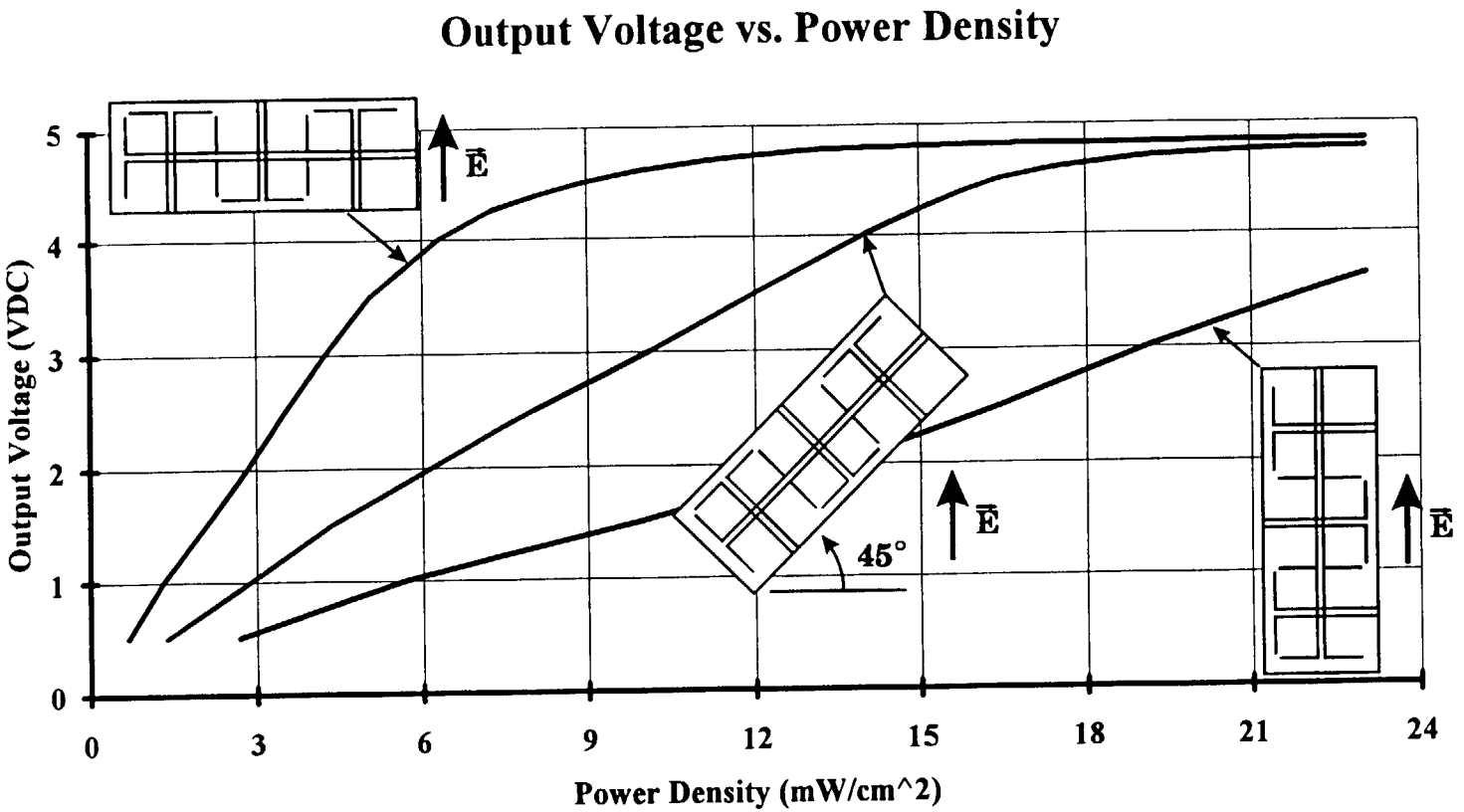


Figure 35. Final assembly performance of the METS rectenna.

**References:**


[1] W.C. Brown, "A transportronic solution to the problem of interorbital transportation," Raytheon Company, Waltham, MA, Tech. Report PT-7452, NASA Contract No. NAS3-25066, July, 1992.

[2] W.C. Brown, "Electronic and mechanical improvement of the receiving terminal of a free-space microwave power transmission system," Raytheon Company, Wayland, MA, Tech. Report PT-4964, NASA Report No. CR-135194, NASA Contract No. NAS 3-19722, Aug. 1977.

[3] W.C. Brown, "Design definition of a microwave power reception and conversion system for use on a high altitude powered platform," Raytheon Company, Wallops Flight Facility, VA, NASA Report No. CR-156866, NASA Contract No. NAS 6-3006, July 1980.

[4] The ARRL Antenna Book, Gerald Hall, Ed. Newington, CT: The American Radio Relay League, p. 3-6.

[5] G.P. Boyakhchyan, V.A. Vanke and S.K. Lesota, "The choice of optimum density of dipoles in a rectenna," Radio Engineering and Electronic Physics (English translation of *Radiotekhnika i Elektronika*), vol. 28, no. 2, pp. 119-122, Feb. 1983.

[6] W.C. Brown, "Free-space microwave power transmission study, combined phase III and final report," Raytheon Company, Waltham, MA, Tech. Report No. PT-4601, NASA Contract No. NAS-8-25374, Sept. 1975.

[7] W.C. Brown, "Rectenna technology program: ultra light 2.45 GHz rectenna and 20 GHz rectenna," Raytheon Company, Waltham, MA, Tech. Report No. PT-6902, NASA Report No. CR-179558, NASA Contract No. NAS 3-22764, March 1987.

[8] K.C. Gupta, R. Garg, and I.J. Bahl, *Microstrip Lines and Slotlines*. Norwood, MA: Artech House, Inc., 1979.

[9] J. McSpadden, T. Yoo, and K. Chang, "Theoretical and experimental investigation of a rectenna element for microwave power transmission," *IEEE Trans. Microwave Theory Tech.*, vol. 40, pp. 2359-2366, Dec. 1992.

[10] W.C. Brown, "All electronic propulsion - key to future spaceship design," in *AIAA/ASME/SAE/ASEE 24th Joint Propulsion Conference*, Paper AIAA 88-3170, 1988.

[11] I.E. Rana and N.G. Alexopoulos, "Printed wire antennas," in *Proceedings of the Workshop on Printed Circuit Antenna Technology*, 1979, pp. 30-1 - 30-38.

[12] A. Alden and T. Ohno, "Single foreplane high power rectenna," *Electronics Letters*, vol. 28, pp. 1072-1073, May 1992